Project N. 037110

NEAREST

Integrated observations from NEAR shore sourcES of Tsunamis: towards an early warning system

Instrument: STREP

Thematic priority: 1.1.6.3 GOCE (GlObal Change and Ecosystems)

D4: Depth-migrated multi-channel seismic profiles

Due date of deliverable: April 2008

Actual submission date: 8th May 2008

Start date of the project: 01/10/2006

Duration: 36 months

Organisation name of the lead contractor for this deliverable: CSIC

Revision: Final

Project Co founded By the European Commission within the Sixth Framework Programme (2002-2006)		
Dissemination level		
PU	Public	
PP	Restricted to other programme participants (including Commission Services)	
RE	Restricted to a gruop specified by the Consortium (including Commission Services	**RE**
CO	Confidential, only for members of the Consortium (including Commission Services)	

WP2 - Tsunami source characterisation

D4: Depth-migrated multi-channel seismic profiles

Task 2.1 Leader:

CSIC

Task 2.1 Responsible:

Valentí Sallarès
Unitat de Tecnologia Marina (UTM) - CSIC
Centre Mediterrani d'Investigacions Marines i Ambientals (CMIMA)
Passeig Maritim de la Barceloneta, 37-49
08003 Barcelona, Spain

1. Abstract

Multichannel seismics (MCS) is considered to be the most powerful geophysical system for imaging the internal structure of the Earth's crust. Its principle is that seismic energy provided by artificial sources (e.g., airguns) is reflected at the geological boundaries showing impedance contrasts such as faults, and these reflections are processed and merged together to obtain continuous images of the sub-surface. MCS has a large number of applications mainly in industry (e.g. hydrocarbon exploration) but also for academic purposes, one of which is the characterization of deep fault and décollement surfaces. This is the case of the MCS profiles shown in this report, selected to provide information on the deep structure of the main potentially seismogenic/ tsunamigenic structures previously identified in the Gulf of Cadiz. MCS data, however, provide images whose vertical axis is time instead of depth. This makes that MCS images are not straightforward to interpret and the correct information on the geometry of the structures imaged must be extracted by means of processing. At present day, the best existing technique to convert the time images into depth sections is pre-stack depth migration (PSDM).

We thus present here a selection of 10 PSDM-migrated MCS profiles acquired in different seismic surveys that have taken place in the Gulf of Cadiz in the last ~15 years: AR-RIFANO-1992; IAM-1994; SISMAR-2001, and SWIM-2006. These profiles provide together valuable information of all the structures that have been proposed as potential sources of the famous Lisbon 1755 earthquake and tsunami. The first is the décollement surface beneath the Gulf of Cadiz imbricated wedge (i.e., the accretionary wedge), which has been suggested to be the inter-plate boundary of an –still- active subduction zone. The second is the Horseshoe-Coral Patch Ridge fault system, which hosts significant seismic activity and is apparently a likely candidate based on recent seismological source modelling. The third is the Gorringe Bank, the major bathymetric feature of the whole area and the main source candidate until tsumani propagation modelling discarded this based on its location. The last one is Marques de Pombal, an impressive thrust fault that is located close to the Portuguese coast. It is too short to explain an Mw 8.5-8.7 earthquake but

seems to be the best suited to explain the timing of the coastal tsunami hit. Finally, we have included depth images of two long ENE-WSW strike-slip fault lineaments that cross almost the whole area. Even if they are not likely sources of the Lisbon earthquake, they display mid-size seismicity and appear to be relevant structures to accommodate plate convergence between Iberian and African plates.

2. Introduction

One of the main problems regarding the assessment of tsunami risk in the Gulf of Cadiz concerns the identification and characterisation of the potential large tsunami sources in the area. It is important to keep in mind that this is the region that hosts the source of the 1755 Lisbon earthquake and tsunami (Abe, 1989), which killed over 60,000 people in Lisbon and several thousands in Cadiz. Although the tectonics of the region is reasonably well understood thanks to the considerable amount of work that has been done in the last ~15 years of continuous research, significant debate in what concerns the most likely sources of the greatest earthquakes (and tsunamis) still remains. This region is described to be composed of 5 distinct structural domains: (1) the SW Iberia and (2) the NW Moroccan continental margins, (3) the thick accretionary wedge in the central Gulf of Cadiz, (4) the deep abyssal plains (Horseshoe and Seine) and (5) bathymetric highs (Coral Patch Ridge, Portimao-Guadalquivir, and Gorringe Banks) showing recent compressional deformation.

The Gorringe Bank, the most prominent bathymetric feature of the area, was initially proposed to be the most likely source for the Lisbon earthquake and tsunami (Fukao, 1973), but tsunami modelling appears to discard it based on its location. More recently, the Marques de Pombal fault system has been put forward as the most likely candidate for the generation of this earthaquake (Zitellini et al., 1999; 2001), although individual fault segments are not long enough to generate an M_w 8.5 earthquake. Other structures considered are the Horseshoe fault, the Guadalquivir-Portimao Banks lineament, and a proposed east-dipping subduction zone beneath the Gibraltar Arc (Gutscher, 2002; Gracia et al., 2003; Terrinha et al., 2003, Zitellini et al., 2004). This lack of consensus is mostly due to the poor knowledge of the geodynamics and the convergence accommodation along the complex African-Eurasian plate boundary (e.g. Grimison and Chen, 1986), the poor correlation between local seismicity and individual faults, and the poorly constrained deep geometry of the main faults identified.

The recent work of compilation made in the framework of the Nearest project, summarized in the form of a new tectonic map based on available multichannel seismic (MCS) and digital terrain models (mutibeam bathymetry, backscatter), has helped to update all the information relative to the main tectonic structures of the area and to shed some light into its history, functioning, and relative significance (Terrinha et al., 2008). Multichannel seismic (MCS) reflection data used in this work have been acquired during successive National and EU funded projects (Figure 2.1) (e.g. Sartori et al, 1994; Banda et al., 1995; Mendes-Victor et al., 1998) with the aim to characterize the shallow structure, and to identify active tectonic sources in the region (e.g. Dañobeitia et al., 1999; Gutscher et al., 2002; Gràcia et al., 2003a,b; Maldonado et al., 1999; Medialdea et al., 2004; Terrinha et al., 2003, Zitellini et al., 2001, 2004). As can be seen in figure 2.1, the MCS data set almost completely covers the region of interest. With the exception of Rovere et al. (2004) and Thiebot and Gutscher (2006), however, MCS profiles have been processed using standard seismic techniques. This means that most of the available MCS profiles have not been depth-migrated, so they do not provide realistic information on the depth and geometry of tectonic structures.

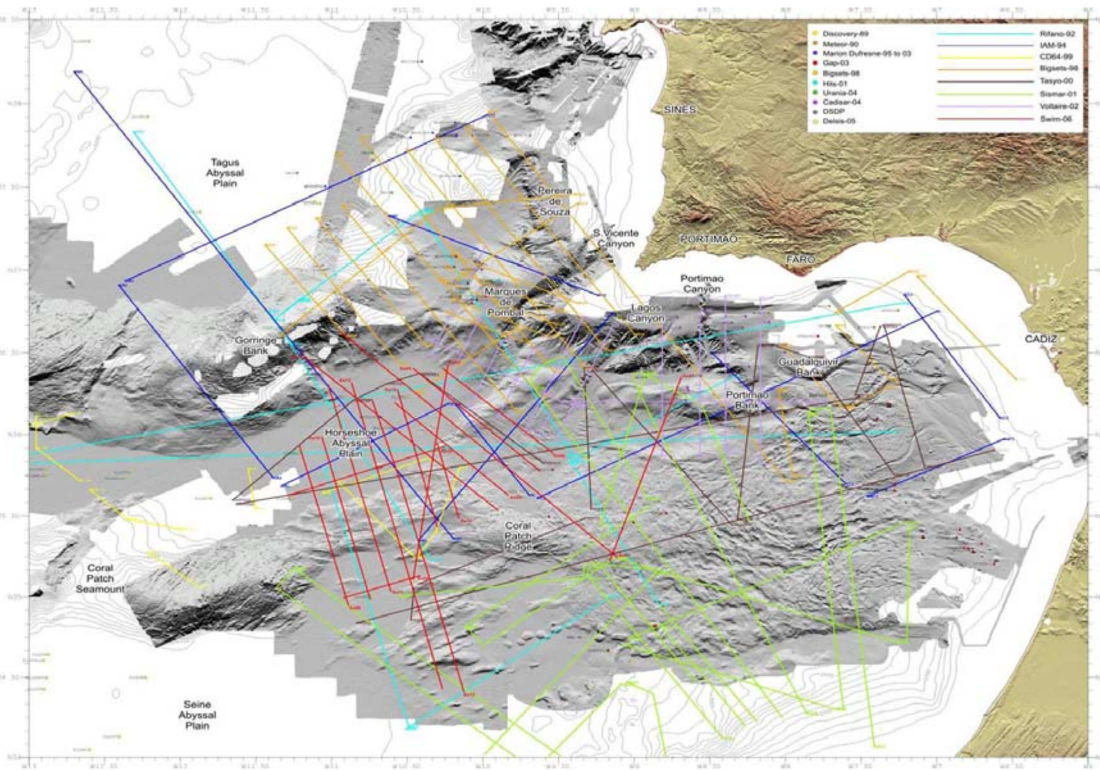

Figure 2.1. *Compilation of all the scientific MCS data acquired in the Gulf of Cadiz during successive cruises since 1992. See legend for cruise identification. Background shaded relief map in grey corresponds to the EuroMargins SWIM bathymetric compilation map (Diez et al., 2005; Zitellini et al., in prep).*

The key goal of task 2.1, and the main topic of this deliverable, is thus to provide accurate images of the tectonic structure as MCS depth sections across the most significant tectonic features, rather than time sections as seismic images are usually interpreted. The purpose is two-fold: on one hand, provide in-depth information about the functioning of the main structures identified in the recent tectonic compilation (Terrinha et al., 2008). On the other hand, provide complementary information to design the best possible location for the OBS-wide-angle seismic profiles that will be shot in October-November 2008 in the framework of the Nearest project. We have in total compiled and re-processed a total of 10 long MCS profiles crossing the most relevant tectonic structures, which were acquired during surveys AR-RIFANO-1992 (2), IAM-1994 (1), SISMAR-2002 (2) and SWIM-2006 (5).

We have organized the rest of the report in four sections. In section 3, we briefly describe the main tectonic domains of the Gulf of Cadiz. In section 4, we present the available MCS data set and we describe the seismic system used to acquire the profiles that have been re-processed. In section 5, we present the methodology used for depth conversion (PSDM) and, finally, in section 6 we show the results obtained as depth sections along the different profiles.

3. Tectonic domains in the Gulf of Cadiz

The Gulf of Cadiz, located offshore SW Iberian Peninsula, is a complex tectonic area that have recorded important historical seismic activity, including the Lisbon earthquake and tsunami (Abe, 1989). According to plate tectonic reconstructions, the southern part of the margin formed during the Jurassic continental break-up between North America and Africa, whereas the western margin formed later, during the Cretaceous separation of Iberia with respect to North America. At present day, the plate boundary (Figure 3.1) trends roughly E-W, connecting the Azores-Triple Junction to the Gibraltar Strait. Its complexity is clearly reflected in the fact that plate motion is divergent east of the Azores, transforms in the middle segment, and is convergent eastward of the Tore-Madeira Ridge. In our study zone (i.e., the area comprised between the Gorringe Bank and the Strait of Gibraltar) compressive stress accommodates NNW-SSE plate convergence at a very slow rate of 4 mm/yr.

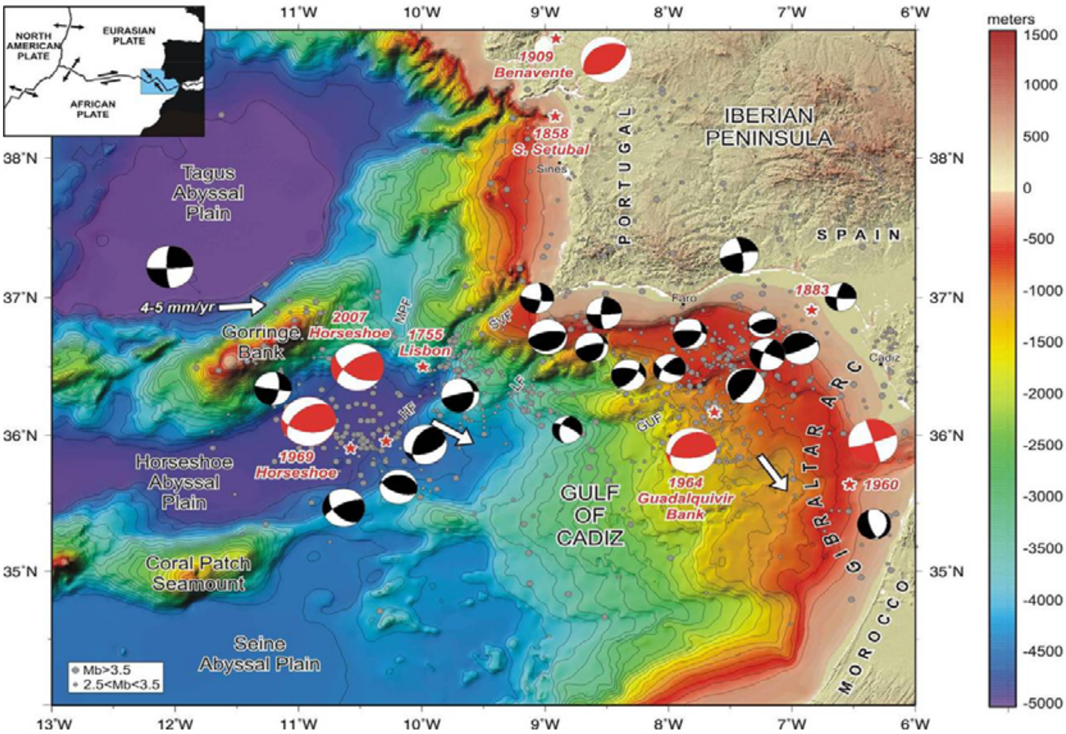

Figure 3.1.- *Topographic and bathymetric map of the Gulf of Cadiz. Presumed plate convergence is depicted by the white arrows. Earthquake epicentres are represented by grey dots. In red, fault plane solutions of magnitude Mw > 6 earthquakes. In black, those of smaller earthquakes (from Stich et al., 2005, 2007). Inset: Plate-tectonic setting of the SW Iberian Margin along the boundary between the Eurasian and African Plates.*

Morphologically, the north (Iberian) and south (Moroccan) margins of the Gulf of Cadiz are partially overburdened by a thick allocthonous body (i.e., the so-called “imbricated” or “accretionary” wedge) related to the neogenic westward migration of the Alboran microplate (Gutsher et al., 2002), and by voluminous olistostromes, discharged gravitationally from the tectonic melange itself (Torelli et al., 1997). These bodies, which globally cover most parts of the basins, mostly hide the seafloor trace of the plate boundary zone. However, the joint interpretation of available swath bathymetry, high resolution profiles and multibeam probe backscatter images have allowed establishing the morphologically different domains and their borders as well as the sources of structural and tectonic control of the buried structures on the present day morphology. In summary, the Gulf of Cadiz shows three main different morphological domains, each of which contains a number of different structures and sub-domains: the Horseshoe Abyssal Plain, the mouth of the South Portugal canyons and the accretionary wedge. The main sub-domains described are summarized in Figure 3.2.

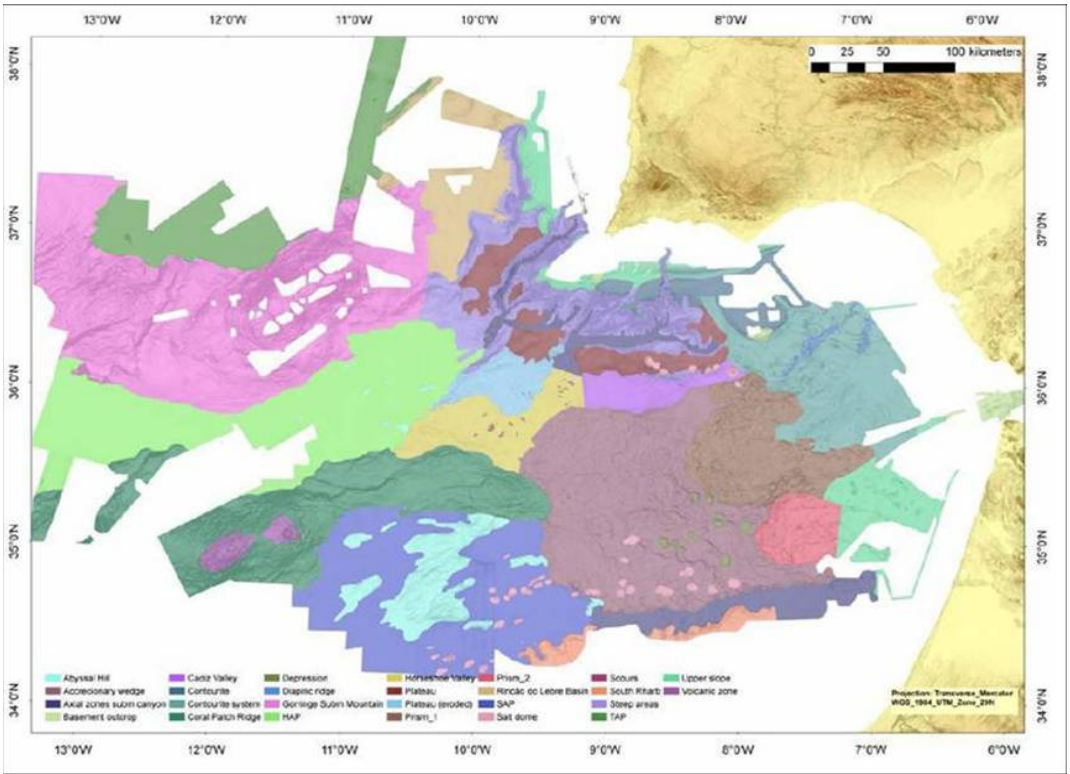

***Figure 3.2.**- Morphotectonic map of the Gulf of Cadiz (from Terrinha et al., 2008)*

From a dynamic point of view, the plate boundary consists of diffuse, active compressive deformation, distributed over a 200-300 km wide area (Sartori et al., 1994; Hayward et al., 1999). Consistently, the seismicity pattern show scattered hypocenters spanning from shallow to intermediate depth (Buforn et al., 1988). Focal mechanisms show a mixture of thrust and strike slip motion. The plate convergence is responsible for the reactivation of the older rifting faults and a number of large, active, tectonic structures have been detected along the continental margin and in the oceanic domain. It is believed that the tectonic reactivation began in the Miocene, although in the Portuguese Margin, the Miocene compression is milder and it is superimposed on an older important tectonic inversion that took place during latest Cretaceous through Paleogene times (Terrinha, 1998). Among the different identified structures, we have considered as active those showing clear evidence of displacement in the Pliocene to present time interval, as explained in the review made by Terrinha et al. (2008). They classified the different structures based on the compilation and joint interpretation of MCS, multi-beam and backscatter data; as well as seismicity data, maps of location of epicenters and hypocenters and computed seismic strain. The resulting compilation is shown in figure 3.3.

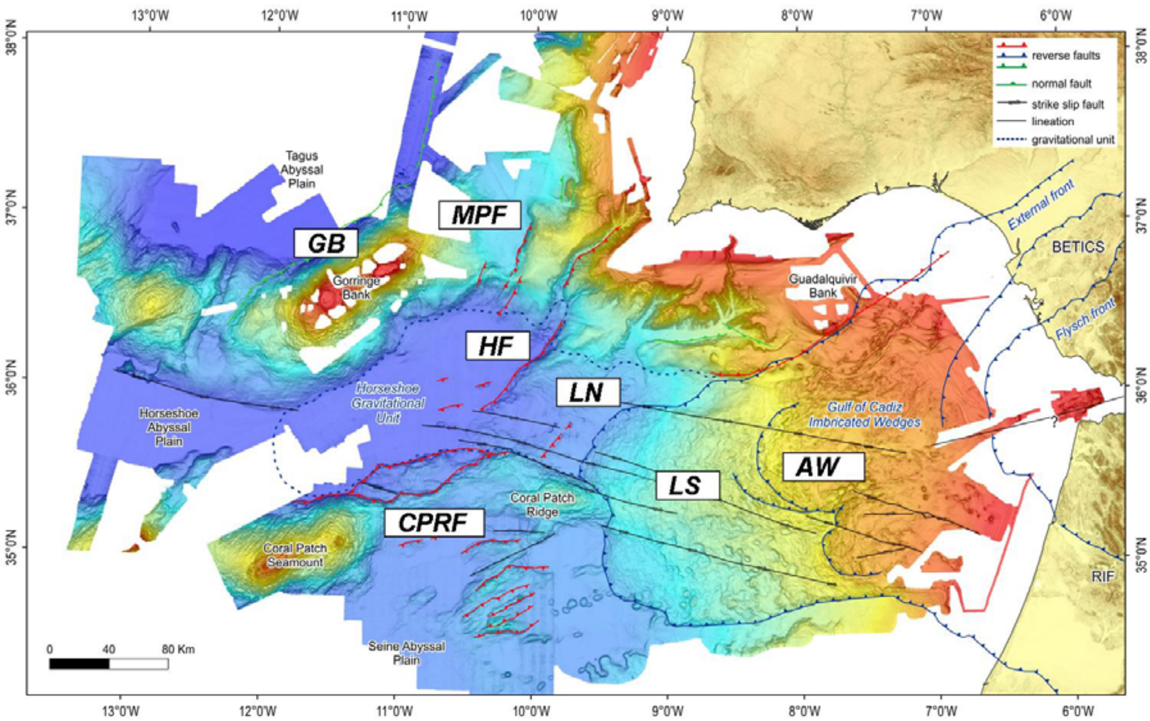

Figure 3.3.- *Tectonic map of the Gulf of Cadiz. See legend for further explanation. AW: Accretionary Wedge; HF: Horseseshoe fault; CPRF: Coral patch ridge fault; MPF: Marques de Pombal fault; GB: Gorringe bank; LN/LS: North and South WNW-ESE lineations.*

According to their classification the main tectonic structures and the associated faults are: (1) The Guadalquivir Structure-Portimao Bank Structure; (2) The Horseshoe/Coral Patch Ridge Fault (3) The so-called “SWIM Faults”; (4) The Marques de Pombal Fault; (5) The Gulf of Cadiz Accretionary Wedge; (6) The Seine Abyssal Fold and Fault System; (7) The Pereira de Sousa Fault; (8) The Gorringe Bank Thrust (Figure 3.3 and 3.4). By comparing this figure with Figure 2.1, it is clear that most of the main active faults identified in the region are crossed by MCS profiles. We have simplified this classification by grouping the faults into meta-systems that are crossed by seismic profiles appropriate to perform seismic processing up to pre-stack depth migration. According to these criteria, the selected tectonic domains and their main characteristics are the following ones:

3.1. The Accretionary Wedge

This designation was first proposed by Gutscher et al. (2002) for a series of seismic chaotic facies body related to the neogenic westward migration of the Alboran microplate, which now displays an eastwards-oriented, tongue-shaped morphology that overburdens most of the eastern part of the Gulf of Cadiz (Figure 3.3). It occupies about 58,000 km^2 of the Atlantic margins of both NW Africa and SW Iberia (Gulf of Cadiz). It has dimensions of around 300 km of length in an ENE–WSW direction and between 150 and 200 km of width in a NW–SE direction. It is of general agreement (e.g. Maldonado et al., 1999, Somoza et al., 2003, Medialdea et al., 2004, Iribarren et al. 2007, Roque 2007) that this body consists of a thrusts complex, which constitute an imbricated cover of sediments that thickens from west to east, reaching a maximum thickness of ~11 km at its eastward edge (Figure 3.4; Iribarren et al., 2007). For this reason it has been also called Gulf of Cadiz imbricated wedge (GCIW). There is also consensus in that the units that compose the wedge were emplaced as a consequence of the NW–SE compression during the north-westwards convergence of Africa. Gutscher et al. (2002) interpreted the eastern part of the Miocene seismically chaotic unit as an active accretionary prism with a western vergence that developed above an east-dipping oceanic subduction beneah the Gibraltar Arc.

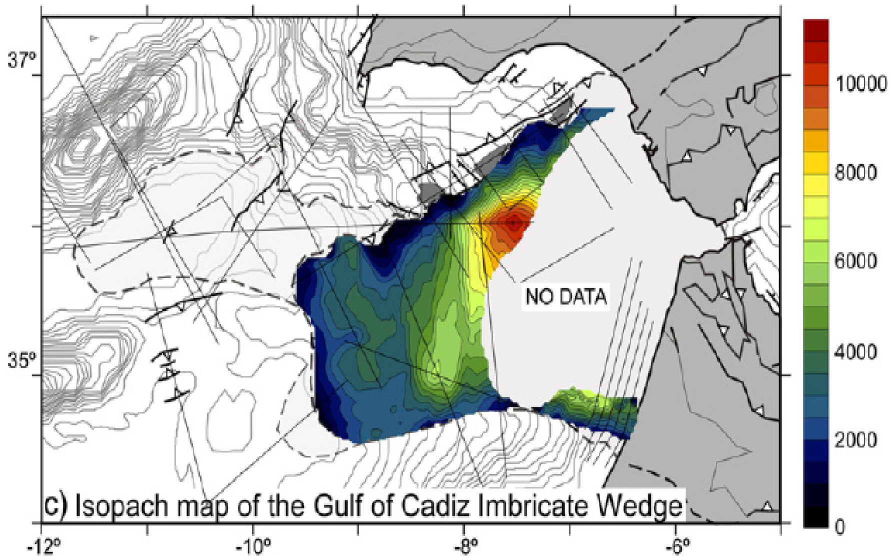

Figure 3.4.-

Isopach map of the GCIW in meters (from Iribarren et al., 2007). The thickness of the unit avoids obtaining an image of the basal surface towards the E.

According to these authors, active subduction would still take place currently beneath the Gibraltar Arc, and most interestingly, it would have been the source of the large 1755 Lisbon earthquake and tsunami. However, as neither active arc volcanism, nor shallow dipping thrust type earthquakes have been observed, the active subduction model is still under debate. Other, indirect evidence will have to be found before this hypothesis could be confirmed.

3.2. The Horseshoe/Coral Patch fault system

The second tectonic domain is that constituted by (1) the main branch of the Horseshoe fault (Gràcia et al., 2003, Zitellini et al., 2004), a reverse fault oriented ~NE-SW, perpendicular to the present day kinematic displacement of Africa with respect to Iberia that separates the Horseshoe Valley from the Horseshoe Abyssal plain; and (2), the “fault and fold” system of the north-western flank of the Coral Patch Ridge/Seamount and the Seine Abyssal plain (Figure 3.3). Although not structurally linked, all the active structures identified in this southern part show also reverse faulting, and are oriented approximately perpendicular to present-day plate convergence, although slightly rotated towards the east with respect to the Horseshoe fault. The north and south parts of this fault system are interrupted and separated by two long WNW-ESE trending lineations (the so-called “SWIM Faults” by Terrinha et al., 2008).

The Horseshoe fault escarpment strongly diminishes from north to south, being the acoustic basement shallower and the fault displacement smaller in the south of the northern lineation than in the north. Most of the scarp is possibly caused by movement on thin skinned thrusting in this segment. The strong geometrical change from north to south has important implication on the interpretation of the fault behaviour and propagation. It is also worth noting that the Horsehoe fault is the site of notable seismic activity, such as the recent February 12th 2007, M_w 6.0, earthquake. It has been also suggested that the inferred source characteristics of the 1755 earthquake are compatible with the moderate length of the reverse faults of the area (such as the Horseshoe one), due to the presence of rigid and cold oceanic lithosphere there (Stich et al., 2007).

The southern "fault and fold" system of the Coral Patch Seamount and the Seine Abyssal plain consist of a series of elongate, SW-NE trending, topographic highs emerging from the flat Seine Abyssal Plain that are controlled by different structures described in the review of tectonic structures. The most significant are rift and inverted rift faults; as well as thrusts and folds related with salt diapirism.

3.3. The Gorringe bank

As mentioned above, and as is clearly reflected in the bathymetric chart, the Gorringe Bank is the most important topographic feature of the area. It is a SW–NE elongated elevation, rising approximately 5 km above the adjacent Horseshoe (SE) and Tagus (NW) Abyssal Plains. The ridge is approximately 200 km-long and 80 km-wide. It consists of two main seamounts: the Gettysburg Seamount in the west, with a minimum depth of 40 m, and the Ormonde Seamount in the east, with a minimum depth of 60 m (e.g. Kazmin *et al.* 1990). The Gorringe Ridge drill site 120 (Ryan *et al.* 1973) clearly shows the basic and ultrabasic composition and the oceanic nature of the rocks in this area. It is considered to be an uplifted block of crustal and upper mantle rocks (Auzende et al., 1978; Auzende et al., 1982; Ryan et al., 1973; Féraud et al., 1986; Girardeau et al., 1998), which forms one of the most prominent gravimetric anomalies of the world, reaching over 400 mGal at the top (Figure 3.5).

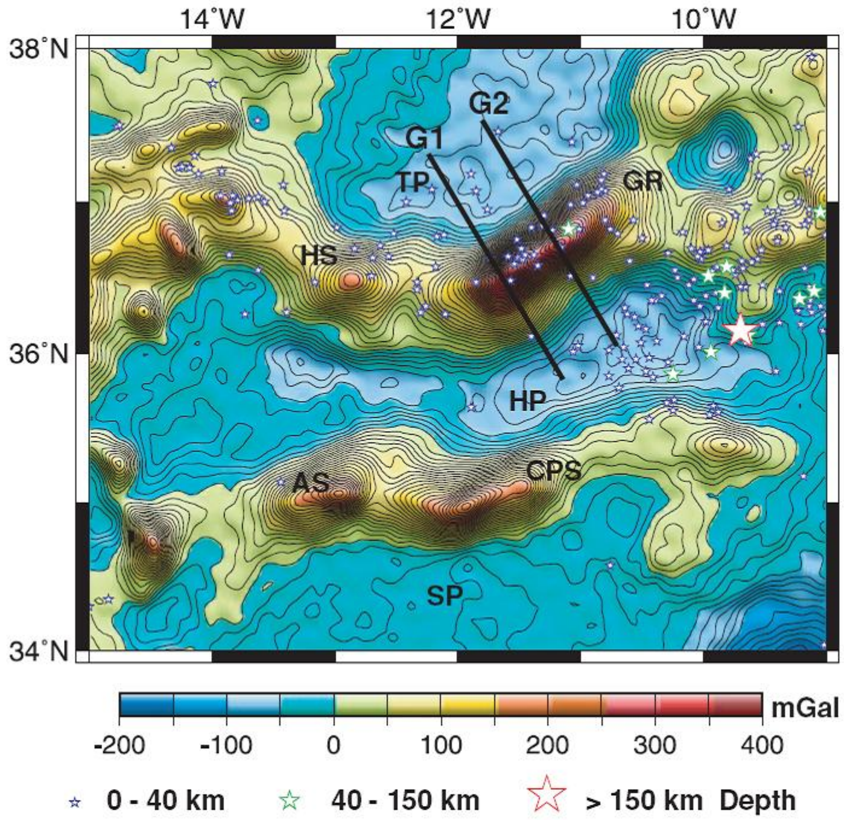

Figure 3.5.- *Satellite-derived free-air gravity anomaly chart of the study area. Contour interval of 10 mGal. Gravity data processed by Sandwell & Smith (1997). Thick lines indicate the location of gravity model profiles in Galindo-Zaldivar et al. (2003). Stars correspond to earthquake epicentre from USGS database (2001). AS, Ampere Seamount. CPS, Coral Patch Seamount. HP, Horseshoe Plain. HS, Hirondella Seamount. GR, Gorringe bank. SP, Seine Plain. TP, Tagus Plain.*

According to Sartori et al. (1994), the Gorringe bank overthrusts the Tagus Abyssal Plain for 4-5 km at least, and shows a strikingly different degree of tectonic deformation to northwest and souteasth. Seismicity indicates that whereas westwards of Gorringe Ridge the plate boundary is located in a narrow zone, eastwards from this area, boundary deformation spreads over a much broader region, more than 300 km wide towards Horseshoe Abyssal Plain (Griminson & Chen 1986).

K–Ar age determinations on gabbros dredged on the Gorringe Bank give values of ~143 Ma, whereas that of the volcanics on the top of the Ormonde Seamount is 60–67 Ma (Féraud *et al.* 1986). The change from deep sea facies of sediments to shallow water facies in DSDP site 120 began approximately 20 Ma (Ryan *et al.* 1973), marking the initiation of the NE-directed over-thrusting. Over-thrusting is considered to have finished during Early Pliocene, but whereas Pliocene-Quaternary sediments show minor deformation associated to the main thrust, it is clearly deformed if compared to the sub-litostrome sediments. This deformation should therefore not be neglected, especially taking into account the notable seismicity associated with the Gorringe Bank (figure 3.5). In fact, it was considered the most likely tectonic source for the 1755 Lisbon Earthquake (Fukao, 1973) until the work of Baptista et al. (1998) suggested that the source zone should trend N-S and be closer to the Portuguese coast.

3.4. The Marques de Pombal fault system

Similar to the Horseshoe fault, Marques de Pombal is a reverse fault trending NNE-SSW that displays a pronounced drag fold at its inner wall. It is located close to the coast of Portugal (< 100 km), and the ridge block is limited to the east by a prominent canyon (S. Vicente) and to the west by a prominent, 50-km long east-dipping thrust fault (Zitellini et al., 1999, Gràcia et al., 2003, Terrinha et al., 2003). It shows higher escarpments in the north (where it reaches maximum a heihght of 1.2 km) than in the south. The northernmost segment is offset by a WNW-ESE wrench fault. The significant activity of this fault is demonstrated by sediment deformation up to Holocene age as observed on high resolution seismic data. Also, the hanging-wall of this thrust displays a fair amount of slides scars and slumps at the seafloor surface (Terrinha et al., 2008). Also associated with this notable fault activity, slope failures and submarine landslides are common all around the block (Gràcia et al, 2003), as explained in deliverable D2 (Review of sources due to slope instabilities). The Marques de Pombal has been recently proposed to be a likely source for the 1755 earthquake (Zitellini et al., 2001), in good agreement with the backward ray-tracing tsunami modelling and shallow-water simulations performed by Baptista et all. (1998).

This fault alone is however too small to generate an earthquake of the estimated magnitude of the 1755 one, even if we consider the simultaneous rupture of a subsidiary thrust fault acting as a back thrust fault. In fact to reach the magnitude of 8.5-8.7 estimated by Mendes-Victor (1990), the hypothesized rupture system should be part of a large area twice as large as the one calculated, so it should involve other faults such as the Horseshoe fault or Pereira da Souza.

3.5. The WNW-ESE fault lineations

The north and south parts of the Horseshoe fault system are interrupted and separated by two long WNW-ESE trending lineations (the so-called “SWIM Faults” by Terrinha et al., 2008) which are strike-slip faults showing important dextral offsets compatible with the dextral kinematics proposed for the region based on the analysis of bathymetric data (Figure 3.6).

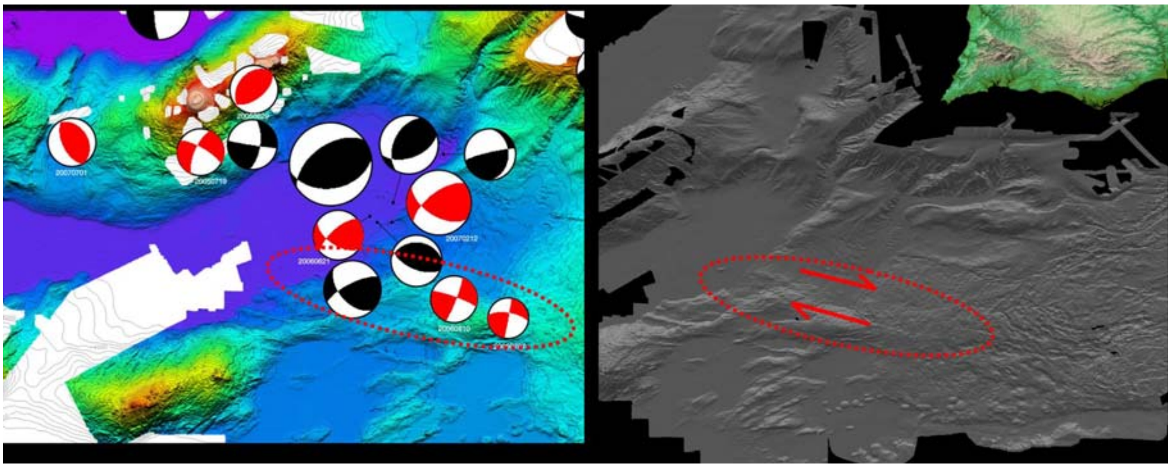

Figure 3.6.- *(left) Detail of the south lineation with recent strike-slip earthquakes superimposed. Focal mechanisms are from Stich et al. (2005). (Right) Detail of the south lineation as indentified in the high-resolution multi-beam bathymetry compilation of the SWIM group (Diez et al., 2005).*

These faults cut across all tectonic structures and geological formations from the Mesozoic basement through the Holocene sediments. They are clearly expressed in the swath bathymetry and also detectable on MCS lines although tracing them down across the chaotic facies is fairly subjective. The longest lineation (the south lineation, figure 3.6) can be easily followed in the bathymetric chart for ~125 km, from the Horseshoe Abyssal Plain up to the Moroccan continental shelf well inside the Accretionary wedge. This fault show recent strike-slip seismic activity as shown in figure 3.6. Although not clearly seen in the seafloor, the fault can be followed based on MCS well to the west of the Horseshoe Abyssal Plain (Bartolomé et al., 2008). The north lineation is shorter (~55-60 km), extending from the Horseshoe Valley and towards the northern half of the “Accretionary Wedge”. It is clear that the WNW-ESE faults offset the Horseshoe Fault and thus it is hypothesized that the WNW-ESE initiated their strike-slip movement during the Miocene. According to their dimensions, it has been suggested that these faults might generate earthquakes of Mw 7.1 (north) and 7.5 (south) using the empirical relationships from Wells & Coppersmith (1994) and Stirling et al. (2002).

Obviously, they are not likely candidates for the 1755 earthquake, and due to its strike-slip behaviour they can neither generate large tsunamis, but they are a relevant source of seismicity in the area that may accommodate significant part of the plate convergence rates. In fact, its WNW-ESE trend matches well the compressional regime between Eurasia and Africa.

4. Multichannel seismic data set

During the last fifteen years numerous academic MCS reflection profiles have been acquired during successive National and EU funded projects with the aim at better understanding the complex plate boundary between Eurasia and Africa and to localize the best candidate source of the 1755 Lisbon Earthquake. The main multi-channel seismic (MCS) surveys that have taken place in the area in this period of time are the following ones: RIFANO (Sartori et al., 1994); IAM (Banda et al. 1995); BIGSETS (Zitellini et al., 2001); HITS; PARSIFAL; TASYO; SISMAR (Gutscher et al. 2002); VOLTAIRE (Zitellini et al. 2004); SWIM (Gracia et al., 2008); MOUNDFORCE (Figure 4.1). The data acquired during these surveys have allowed together to identify a considerable number of active tectonic structures in the region (e.g. Dañobeitia et al., 1999; Gutscher et al., 2002; Gràcia et al., 2003a,b; Maldonado et al., 1999; Medialdea et al., 2004; Terrinha et al., 2003, Zitellini et al., 2001, 2004), some of which have been proposed as likely sources for the 1755 earthquake. As can be seen in figure 4.1, the MCS data set covers most of the region of interest.

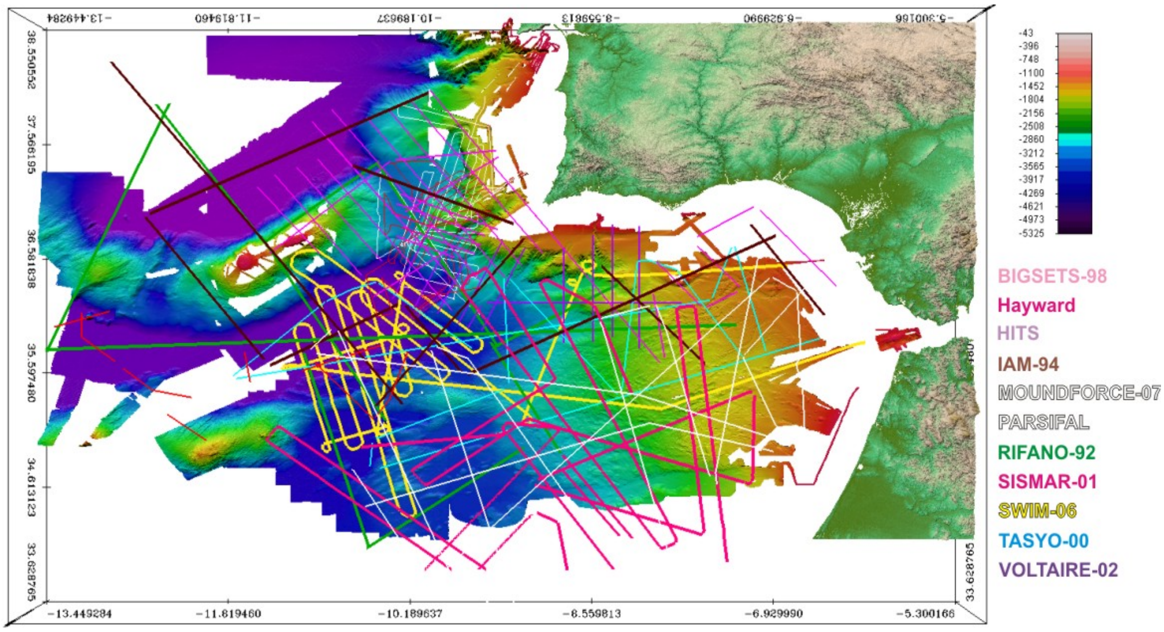

Figure 4.1.- *Multibeam bathymetric map of the study area with all the MCS lines that has bee acquired during the last 15 years (see legend for cruise identification).*

Out of the numerous MCS profiles available in the different surveys, we have selected 10 corresponding to the AR-RIFANO-1992 (2), IAM-1994 (1), SISMAR-2002 (2) and SWIM-2006 (5) surveys for depth migration. The reason for this is two-fold: on one hand, these profiles have a good quality that permits obtaining clear depth-images of the different structures up to 8-10 km deep. This is due to the appropriate acquisition systems for deep seismic sounding that were used in these surveys. On the other hand, the profiles that have been selected cross, as a whole, most of the major tectonic structures in the five tectonic domains described in the previous section, so they are representative of the most potentially dangerous structures of the region. In fact, all the candidate sources proposed for the 1755 earthquake and tsunami are crossed by at least one of the profiles shown here.

In the following sections we briefly describe the characteristics of the acquisition system used in these four surveys as well as some details of the pre-processing made.

4.1. Rifano-1992 Survey (AR)

Rifano-1992 was the first academic multichannel deep seismic reflection survey that took place in the Gulf of Cadiz area. It was shot in July 1992 and the project PI was R. Sartori (U. Bologna). It was acquired by the Italian CNR using the facilities of the R/V OGS Explora of the Osservatorio Geofisico Sperimentale of Trieste. The long acquired lines covered the whole region, including the Gorringe Bank, Marques de Pombal and Horseshoe faults, and the seismically chaotic body (i.e., the accretionary wedge), yielding information on its geometry, structure, and substrate (Figure 4.2) (Torelli et al., 1997).

The energy source was generated by a 32 airgun-array with a total capacity of 80 L. The data were acquired with a 3000 m-long, 120-channel streamer with hydrophone groups separated 25 m from one another. The shot interval was 50 m, and data were gathered to produce 12.5 m common depth points (CDPs) with a 30-fold coverage. The seismic data were recorded on a SERCEL system to 13 s (14 for line 1) at a 2 ms sample interval. Demultiplexing was carried out on broad (Sartori et al 1994). The processing was done at the Istituto di Geologia Marina of Bologna using the commercial package “DISCO”.

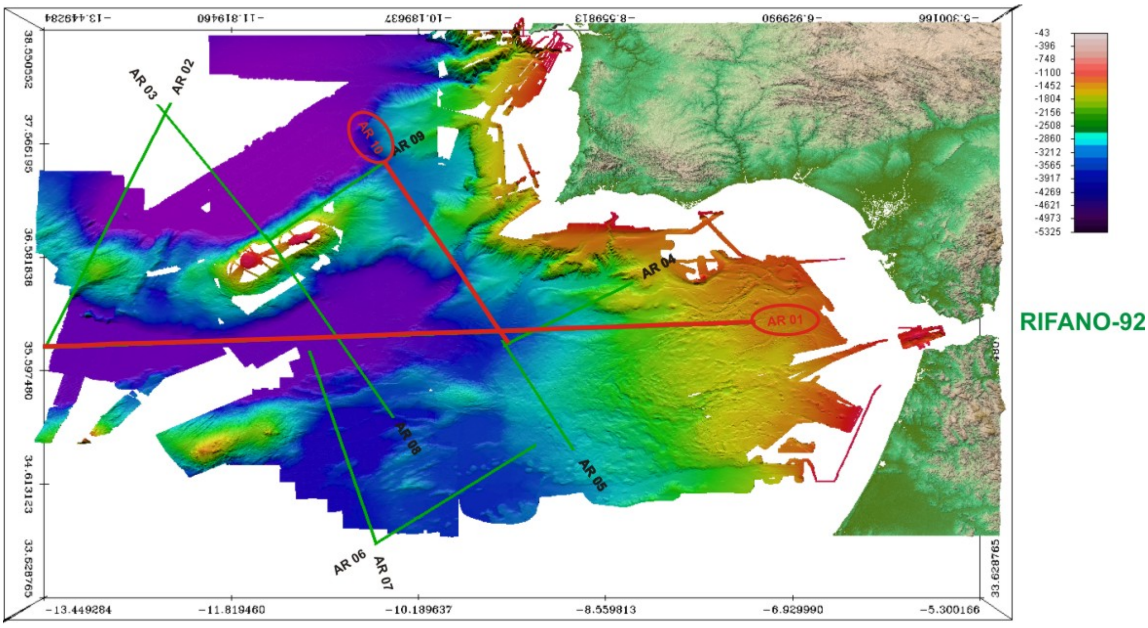

Figure 4.2.- *Lines acquired during Rifano-1992 MCS survey. We have highlighted in red the profiles that were selected for PSDM (AR01 and AR10). These profiles are shown in sections 6.1 and 6.2.*

The two profiles incorporated to this deliverable are AR01 and AR10 (Figure 4.2). AR10 is 250 km long, runs NW-SE, and crosses the Marques de Pombal Fault north of Gorringe Bank, whereas AR10 has a total length of 500 km and runs E-W from south of the Hirondelle seamount to well inside the Accretionary Wedge at 7º W. AR10 and the westernmost 275 km or AR01 were reprocessed at the Ifm-Geomar Seismic Processing Center up to time migration and Kirchoff pre-stack depth migration (PSDM). A description of the method details is included in section 5 of this report. The pre-processing included trace editing, amplitude balancing, normal move-out correction, common-midpoint stacking, predictive deconvolution, finite difference time migration and time variant band-pass filtering. Finally the profiles were iteratively pre-stack depth migrated to 18 km in depth and focusing error analysis was performed every 200 CMPs to create the velocity model.

4.2. IAM-1994 Survey (IAM)

During fall 1994, the UE-funded IAM (Iberian Atlantic Margins) survey was carried out. The PI of the experiment was E. Banda (CSIC), and the survey was run by the company Geco-Prakla using the facilities of its seismic vessel Geco-

Sigma (Banda et al., 1995). During the cruise, over 3,800 km of deep multichannel seismic reflection lines were acquired in the western continental margins of the Iberian Peninsula, from the Cantabric margin to the Gulf of Cadiz (Figure 4.3). The energy source used was a 36 airgun-array, composed of 6 groups, with total air volume of 7524 in^3 at a nominal pressure of 2000 psi. The shot spacing was 75 m in most of the lines although a few lines (i.e., IAM-2W) were shot at 150 m. The main data acquisition parameters were a streamer of 4.9 km, with 196, 25 m-spaced, channels constituted of 40 hydrophones each, giving therefore a maximum fold of 32. Airgun shooting was also recorded by portable seismic stations located onshore, as refraction/wide-angle reflection seismic lines (Banda et al., 1995; Gonzalez-Fernandez et al., 2001).

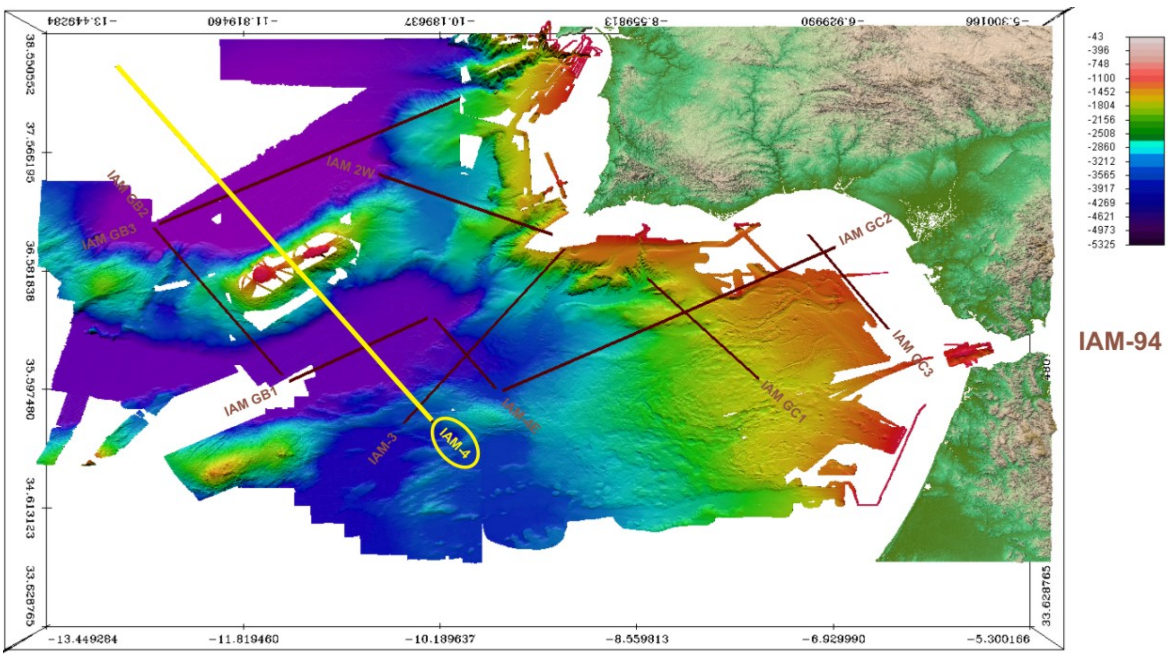

Figure 4.3.- *IAM-1994 survey MCS lines that were acquired in the SW Iberia margin. We have highlighted in yellow the IAM-4 profile, which has been included in this report compilation (section 6.3.)*

The profile selected to be included in this report is IAM-4, which is more than 400 km-long and crosses the Gorringe Bank from the Tagus to Horseshoe Abyssal Plains up to the Coral Patch Ridge. Similarly to Rifano profiles, IAM-4 was re-processed at the Ifm-Geomar Seismic Processing Center up to time migration and Kirchoff pre-stack depth migration (PSDM) (L. Pinheiro, personal communication). The processing sequence and method is described in chapter 5.

4.3. SISMAR-2001 Survey (SIS)

The SISMAR seismic cruise was run in April 2001. The PIs were J. Malod and P. Réhault (UBO), and it was made with the French Nadir oceanographic vessel. The main objective was to image the deep structure of Moroccan margin, to characterise the nature of the crust in the transitional domain and define the geometry of syn-rift basins (Contrucci et al., 2004). Also, several profiles were shot on top of the "Accretionary Wedge", with the aim at better constraining the geometry and nature of the crust beneath the allocthonous body (Thiebot and Gutscher, 2006). A total of 24 deep seismic sounding lines simultaneous with 48 OBS refraction records were acquired during the cruise (Figure 4.4.)

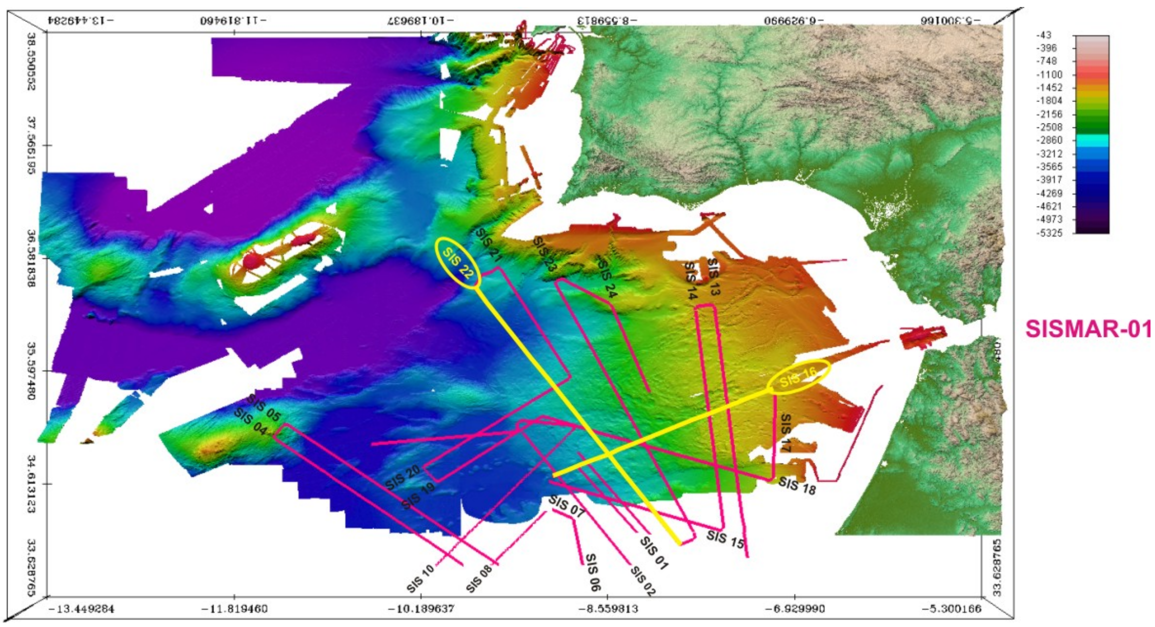

Figure 4.4.- *SISMAR-2001 survey MCS lines that were acquired in the SW Iberia margin. We have highlighted in yellow SIS-16 and SIS-22 profiles, which have been included in this report (section 6.1)*

The acquisition system was a digital, 360 channel, 4.5 km long streamer and a 4805 c.i. tuned airgun array. The streamer was towed 225 m behind the ship at 20-m depth and recorded the signal over a 20-s window, at a 4-ms sampling interval. Shot spacing ranged from 75 m (for purely MCS profiles) to 150 m (for joint OBS and MCS profiles). This provided 30- and 15-fold CDP coverage, respectively. Thus, CDP spacing was 6.25 m for the MCS only profiles and 12.5 m for the joint profiles. Processing of the MCS data was performed using the GEOVECTEUR processing package. In this compilation we have included MCS profiles SIS-16 and SIS-22 (Figure 4.4), which give information on the structure and fault geometry beneath the wedge. The profiles were also PSDM at the Ifm-Geomar Seismic Processing Center. The processing sequence included a standard sequence of static correction, time and space variant, band pass frequency filters, and a spherical divergence correction. Next a minimum delay transformation was applied because the airgun array was tuned to single-bubble mode (not minimum phase), so the source wavelet had to be minimum phase-converted to apply deconvolution (Bartolomé et al., 2004). Deconvolution was then performed to reduce the bubble reverberations. Inner trace muting and f–k filtering were applied in order to attenuate the multiple. Thereafter, a velocity model was constructed iteratively by focusing analysis as in the case of the previously described data.

4.4. SWIM-2006 Survey (SW)

The ESF-EuroMargins SWIM MCS cruise took place in June 2006 on board the Spanish RV Hespérides (Figure 4.5). The PI of the project was E. Gràcia (CSIC). The aim of the seismic survey was characterizing the geometry, deep structure and timing of deformation of the active faults located at the westernmost Gulf of Cadiz (SW Iberian Margin), and especially the Horseshoe/Coral Patch Ridge system. During the cruise sixteen multi-channel seismic (MCS) profiles together with swath-bathymetry and sub-bottom profiler data were acquired.

Seismic acquisition was performed using an array of 8 airguns towed at 6 m depth with a total volume of 1050 c.i. (17.2 L) at a pressure of 2000 psi. To trigger and synchronize the gun array, a “Minipulse” gun controller was used. To record the MCS data was used a Teledyne analogue streamer, with 2,4 km of active section (24 active sections of 100 metres each) towed at 7 m depth. Each of the active sections was configured to form 4 channels with 24 hydrophones per channel, totalizing 96 channels separated 25 m from one another. Sampling rate was 2 ms. The record length was 11 s with a shot distance of 37.5 m, giving a maximum CDP fold of 32. Only the first profile (SW-01) located in a shallower area, was recorded with a length of 9 s and shot interval every 25 m, for a fold of 48.

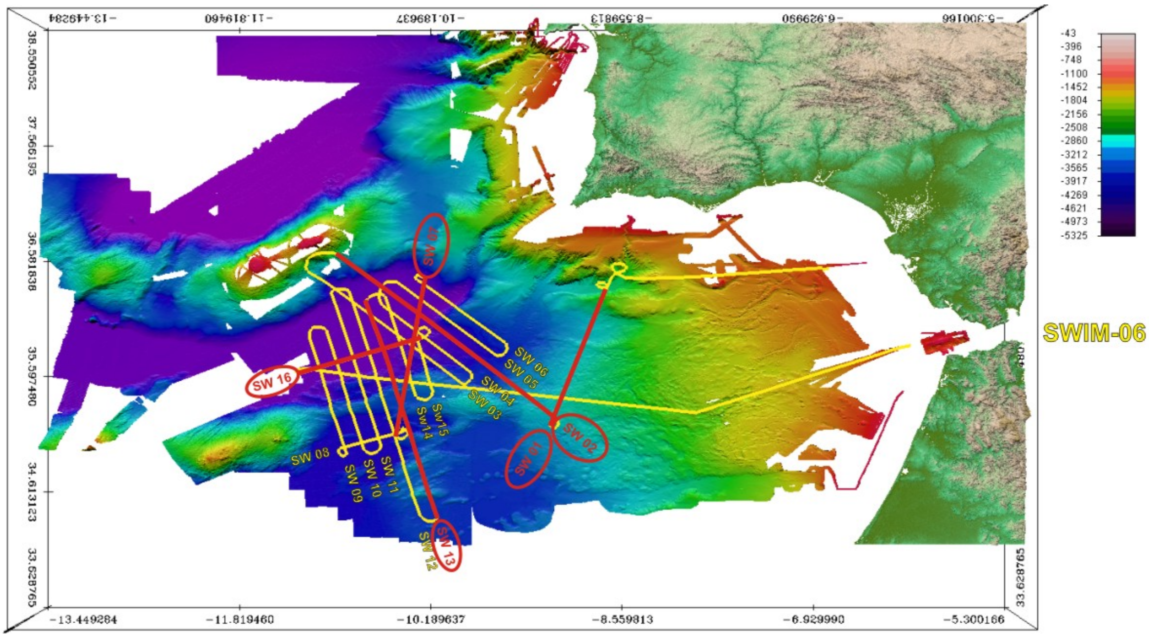

Figure 4.5.- *SWIM-2006 survey MCS lines that were acquired in the Gulf of Cadiz region. We have highlighted in yellow SW-01, SW-02, SW-07, SW-13 and SW-16 profiles, which have been included in this report (sections 6.2 and 6.5.)*

The selected profiles are SW-01, cutting almost perpendicular to the North and South lineations, SW-02, cutting the S lineation as well as the Horseshoe fault, SW-07 and SW-13, cutting the Coral Patch Ridge, and SW-16, perpendicular to SW-13 in the Horseshoe Abyssal Plain. Standard MCS processing was done using PROMAX software. Data was re-sampled from 2 to 4 ms in order to half the size of dataset. Every channel has a static correction of 59 ms due to the existing lag between the recording window and shot triggers. Top mutes were picked in the shot gather domain. A true amplitude recovering was applied to the shot gathers in order to increase the amplitude arrivals due to geometrical spreading looses. Fx-decon was applied in order to filter the individual noise to enhance the lateral continuity of the geological structures. Ensemble predictive deconvolution (pre-stack; 300ms operator length, 30ms prediction lag and 10% white) was applied trying to reduce reverberation and other short period multiples within the data. The ship navigation was corrected binning to CDP sorting (fold: 25-33; bin: 12.5; min. offset: 105m; source depth: 6m; receiver depth: 7m). After CMP sorting, a velocity model for Kirchoff depth migration was performed at the Ifm-Geomar Seismic Processing Center as in the other cases.

5. Methodology: Pre-Stack Depth Migration

Un-migrated time images are not accurate geometric representations of the Earth sub-surface because they are distorted, contain diffractions associated with faulting, and thus do not provide proper information about its real depth and geometry. It is therefore crucial to solve this and place the horizons at their correct depth and dip in order to correctly interpret the images, quantify the fault's recent offsets and to use the structure as input for tsunami modelling. The strategy most commonly used is to analyse and re-process the seismic reflection data and perform what is known as pre-stack depth migration (PSDM). PSDM takes into account ray-path bending and thus corrects for distortions caused by laterally variant velocity structures, providing the correct depth image of complex structures, including faults. The goal of migration is to make the stacked section appear similar to the geologic cross section along the seismic line. Migration moves dipping reflectors into their true subsurface positions and collapse diffractions, thereby delineating detailed subsurface features such as fault planes. In fact, it is not necessary to have complex structures to take advantage of migration: occasional disruptions of reflection continuity, which give rise to diffractions due to growth faults, that are subtle on the stacked section, become apparent on the migrated section. The clarity of the migrated section is preferable not only for geometrical reasons but also to interpret the image (Figure 5.1).

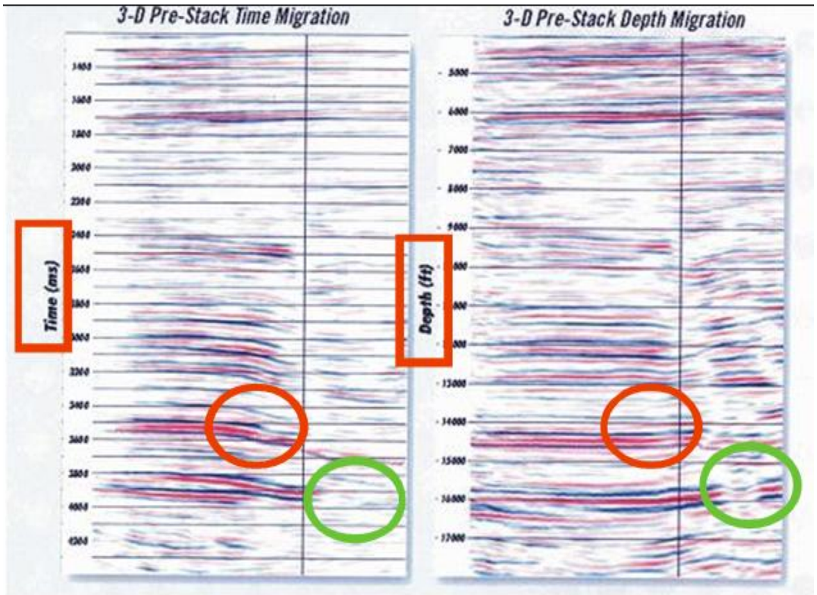

Figure 5.1.- *In the pre-stack time migration (left panel), seismic reflectors on the up fault-block display classic fault shadow "sag" (red circle). In the pre-stack depth migration image (right panel) the same reflectors are correctly positioned. Also, reflectors on the down side of the fault (green circle) are better focussed in the depth image, thanks to correct modelling and imaging with a good velocity field.*

Migration does not displace horizontal events; it moves dipping events in the updip direction and collapses diffractions, thus enabling fault delineation. Taking into account that the main goal of the acquisition surveys in the Gulf of Cadiz is the study of active structures and faults, the migration of the seismic sections become necessary. Correct migration requires an accurate velocity model, but getting the appropriate velocity model is a though task. In fact, the lack of a correct velocity model is generally the most important factor that prevents applying migration to move dipping events to its correct position.

Moreover, a problem that always affects geologists and interpreting geophysicists is the fact that seismic data are displayed in time rather than depth (Figure 5.1). The vertical exaggeration changes with depth (because velocity usually increases with depth) thus distorting the perspective and changing the apparent dip of faults planes.

We can describe the geometric variations of a reflector during the migration process by comparing this reflector in the geological section and in that of time. By making this comparison it is clear that:

1. The dip angle of the reflector in the geologic section is greater than in time section; thus, migration steepens reflectors

2. The length of the reflector, as seen in the geologic sections, is shorter than in the time section; thus, migration shortens reflectors.

3. Migration moves reflectors in the updip direction.

5.1 Type of migrations

Time and depth migrations: The migration process that produces a migrated time section is called *time migration*. Time migration is appropriate as long as lateral velocity variations are mild to moderate. When the lateral velocity gradients are significant, time migrations dos not produce the true subsurface image. Instead, we need to use depth migration, the output of which is a depth section.

After stack (post-stack) and before stack (pre-stack) migration: The migration could be also pre and post stack. When a stacked section is migrated, we use the *post-stack migration*. The post-stack migration uses the theory applicable to data recorded with a coincident source and receiver (zero-offset), that is, the theory for the concept of stack where we assume that a stacked section is equivalent to a zero-offset section. In other words, during the stack we collapse the offset (horizontal) axis by stacking the data onto the midpoint-time plane at zero offset assuming hyperbolic “moveout” (Yilmaz, 1987).

Because of the presence of strong lateral velocity variations, the hyperbolic assumption may not be appropriate for some reflections on some CMP gathers. The assumption that a conventional stack section is equivalent to a zero-offset section also is violated in the presence of strong multiples and conflicting dips with different stacking velocities. If the assumption is not valid, we cannot use post-stack migration. This is the case for reflections occurring at the same time with different stacking velocities: when a flat event is intersected by a dipping event, we can only choose a stacking velocity in a favour of one of these events, not both, and then the stacking process degrades the quality of the image. Thus, in the presence of conflicting dips, stack no longer is equivalent to a zero-offset section and we must use *pre-stack depth migration (PSDM),* where a migration of unstacked data is performed.

The most common way of doing PSDM (and the one that has been used with the profiles shown in this report) is that known as Kirchhoff summation. It is based on the nonzero-offset traveltime equation for a point scatterer. Instead of summing along the zero-offset diffraction hyperbolas (as the post-stack migration), amplitudes are summed along the nonzero-offset diffraction traveltime trajectories (Yilmaz, 1987). As with the zero-offset case, the velocity field dictates the curvature of these summation paths. Each common-offset section is imaged separately in this way and the results then are superimposed (stacked) to produce the migrated section. Clearly migration pre-stack produces a superior section because all dips are present in the section. Although we can solve the conflicting dips problem by the migration before stack, other problems are associated with this approach, namely (1) it is expensive in terms of computation complexity, and (2) it is very sensitive to errors made in the velocity field determination. These errors are most severe at steep dips, precisely where migration before stack should be most useful, making sometimes the migrated section difficult to interpret due to unfair migration derived from erroneous velocity.

The exponentially increasing computational power made PSDM to become a common tool not only in industry but also in academia. The biggest challenge to carry out PSDM has been transferred from the time required to complete each migration step to find a good model of velocities, especially in complex environments where salt sheets distort the seismic raypaths and mask the detection of underlying geology. PSDM is recognized as the only technique available to image through the salt to define subsalt reservoirs, thanks to the improvements in the image quality and a shorter turnaround time.

Areas of geological complexity such as salt bodies, shallow gas-charged zone, rugged water bottom, faulted blocks, steep dips need a priori the application of PSDM. As explained in the previous sections the Gulf of Cadiz seafloor show large structures showing active thrusts, normal and strike-slip faults that are the object of this study. To image these structures properly at depth using MCS data, PSDM is indubitably the most appropriate tool.

5.2. Data pre-processing

Pre-processing the data before the PSDM is essential. Everything from geometry definition through demultiple should be done with care. The presence of noise can mask the desired image and PSDM is very sensitive to noise.

Therefore, extensive noise reduction and careful application of signal enhancers must be applied prior to the initial migration (Figure 5.2).

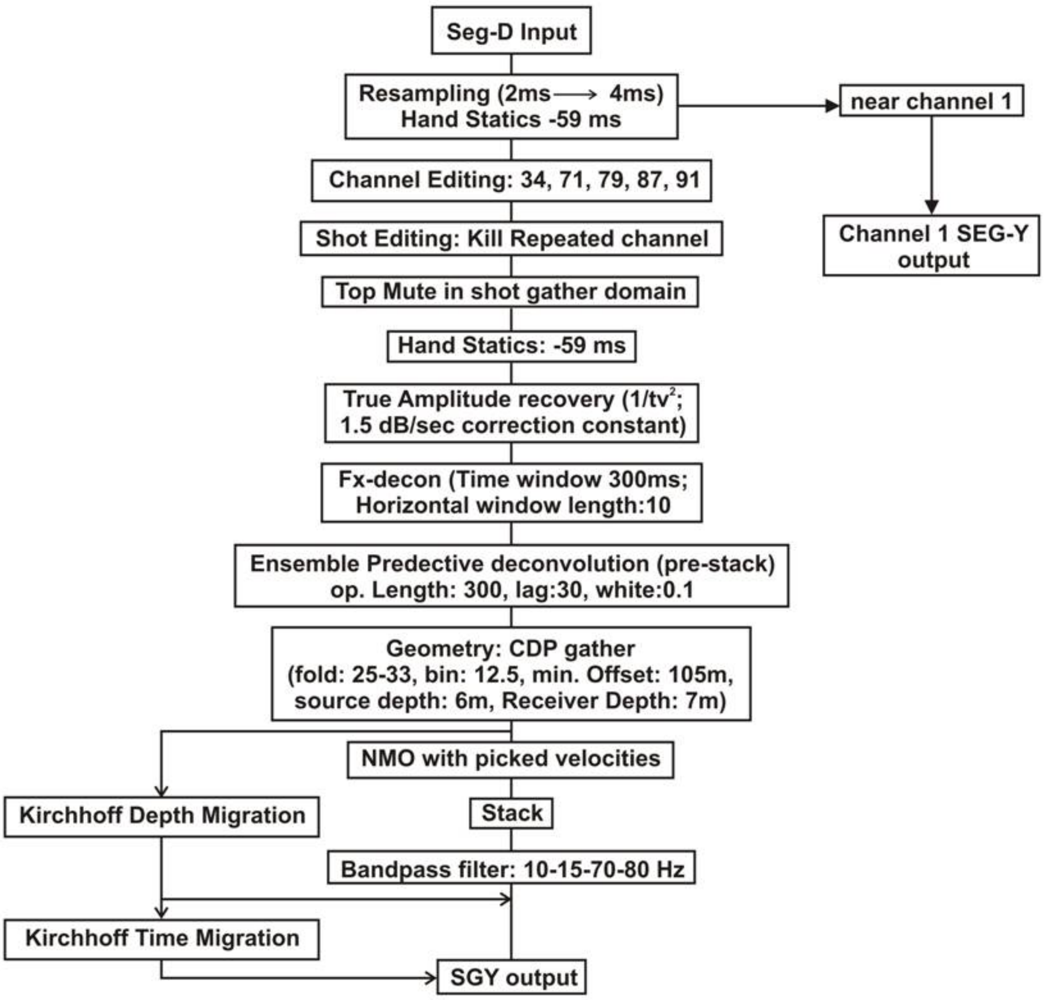

Figure 5.2.- *Flow of seismic processing applied to the SWIM-2006 MCS data*

All the PSDM profiles presented here have been processed at the Ifm-Geomar Processing Center. With slight differences the pre-procesing sequences have consisted on the next steps: we started the noise reduction carrying out the edition of traces and repeated channels. Then, we have enhanced the signal. The seismic wave front loses energy as it propagates through the Earth as a result of absorption, transmission/reflection losses and geometrical spreading. To compensate the loss of energy, we have used a true amplitude recovery by applying a time and space variant gain to the raw seismic shots using a velocity field. We have removed low frequency noise bursts clearly visible in the data as a result of the sea-swell over the streamer using a band-pass filter. In some of the lines we also applied a FK filter in order to remove some distinct dip noise. The F-K filter can be a source of problems if it is applied in an incorrect way, since it can delete signals coming from dip events at big offsets when confusing them with a dip noise (Figure 5.3).

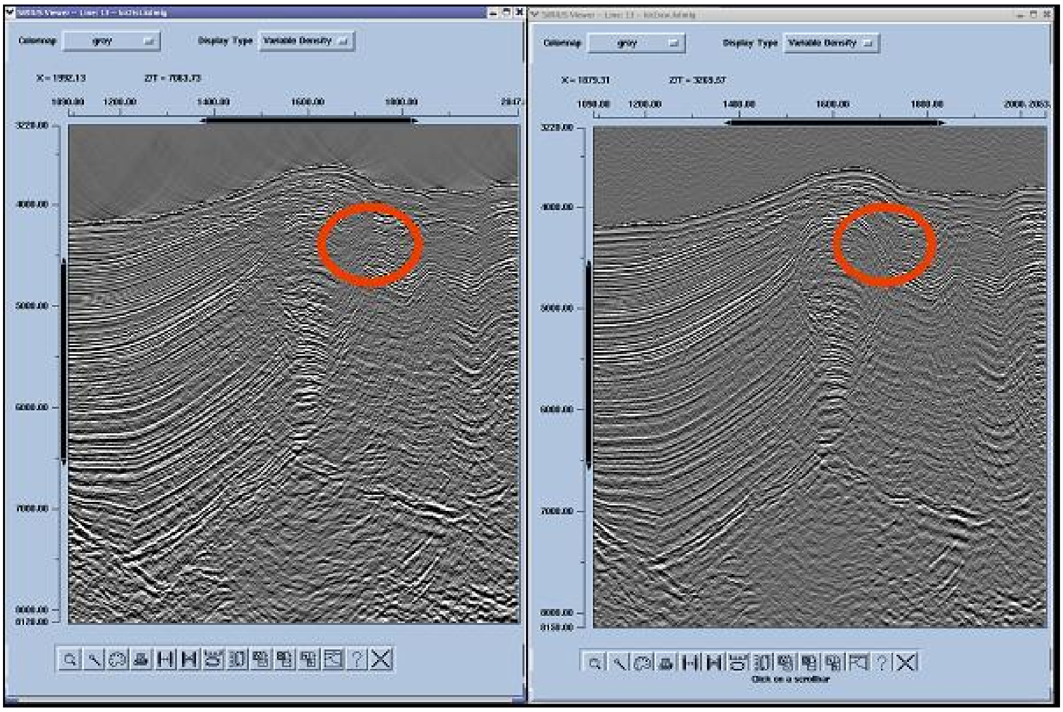

Figure 5.3.- *Zoom area in the pre-stack depth migration of line SW13. To apply a bad designed F-K filter before the pre-stack depth migration can delete the structure (left panel) that we can observe in a non F-K depth migration (right panel).*

The second major pre-processing step is the deconvolution before stack to reduce the reverberation of the arrivals. We have used predictive deconvolution. We have tested the two parameters that control the deconvolution, the operator length and the gap, with the autocorrelation of the signal.

Multiple removal and discrimination are especially important in areas of fault tectonics and with small water column. In this case, multiple arrivals come at the same time of primary with a different dip. Although we could probably suppress most of these multiples just by stacking with the correct velocity, it is hard to see the primary arrivals in order to pick the correct velocity ans suppressing it.

5.3. Definition of the velocity model

Accurate velocity definition is the key factor in PSDM: the quality of the final image is related to the construction of the velocity model. The method followed at Ifm-Geomar to construct the velocity model is known as depth-focussing error analysis of the MCS data. We have used the SIRIUS software package (GX Technology). This package includes PSDM (although it can be run with any other software once the velocity model is performed) with depth-focussing analysis based on finite-difference and ray-tracing algorithms (McBarnet, 2000). The velocity model is constructed layer by layer iteratively. Since velocities generally increase with depth, errors in migration are usually larger for deep events than for sallower ones. Also, the steeper the dip, the more accurate the migration velocities need to be, since displacement is proportional to dip.

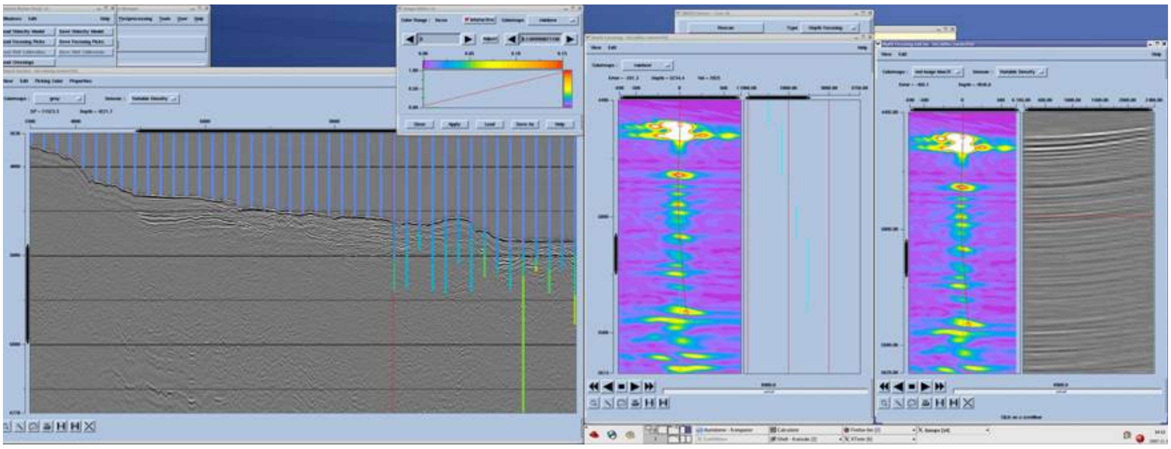

Figure 5.4.- *Panels used for the velocity picking in the third iteration. In the left panel, the pre-stack depth migration obtained in the previous iteration and in a new horizon the velocities are being picked. In the central panel, velocity focussing analysis showing the energy concentration in a semblance display and the value of the interval velocity picked in white vertical lines. In the right panel, the same velocity focussing analysis of the central panel and the CMP gathers overcorrected ("smile" shape): we need to reduce the velocity.*

The first iteration to obtain the velocity model begins with the water velocity to replace the seafloor in depth. In the next iteration the processor, interpreting the section, defines a new horizon (usually the clearest and most continuous reflector) where new migration velocity analyses are performed in some specified CMP positions (usually frequent intervals to obtain a homogeneous velocity field). These analyses consist in various attempts at migration with different velocities and place them side by side, producing a display of envelope of velocity (or semblance) versus depth. In practice, the processor has to pick the maximum semblance focussing velocity (where the energy is focussed) in the velocity vs depth display and the software, to improve the quality of velocity picks, perform the velocity analyses from a number of neighbouring CMP gathers often summed (Figure 5.4).

By this way, a new run of migration can be done with the new velocity model that will migrate properly until the horizon picked. The result is the input for the next iteration where a new horizon is chosen and new analyses can be done. Each iteration becomes increasingly accurate as interval velocities and structure becomes clarified. This iterative modelling is strongly coupled with geological interpretation (horizons). Thus lateral velocity variations are defined and the depth structure is revealed itself. As the final structure/velocity model is confirmed, the depth-focussing errors are close to zero for all depths. The final velocity model used for the PSDM is shown over the section in figure 5.5.

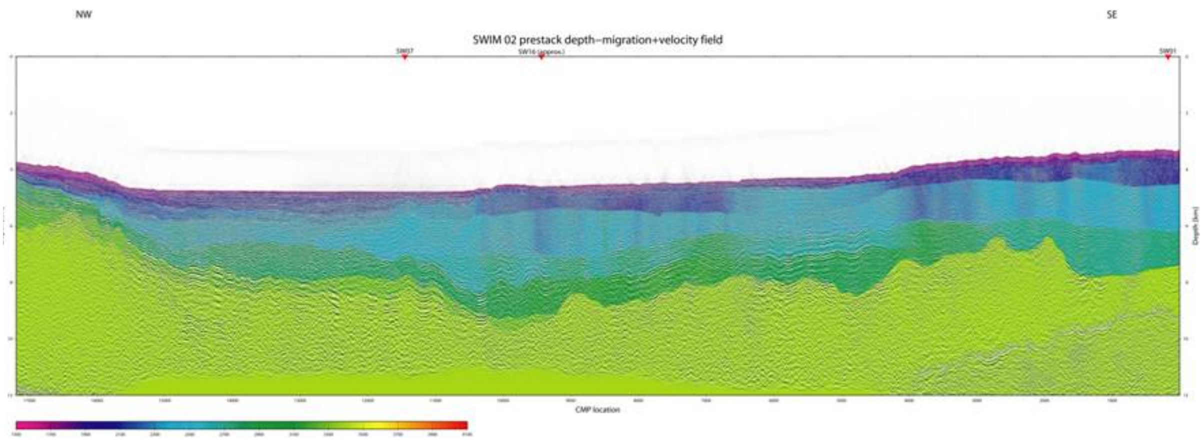

Figure 5.5.- *Pre-stack depth migration with the final velocity field used for the last iteration in profile SW02 (SWIM-2006 survey).*

6. Results

In the following sections we present depth-sections of the selected profiles. The images shown correspond to stacked sections, Kirchoff PSDM-migrated sections, as well as the velocity model obtained from iterative error focussing analysis (when available). The location of the seismic profiles is shown in the different figures of chapter 4. Each of the selected profiles crosses one (or several) relevant, potentially seismogenic/ tsunamigenic structures, representative of the five different tectonic domains described in chapter 3.

6.1. The Accretionary Wedge (SIS-16, SIS-22)

The record sections corresponding to the profiles located over the so-called "Accretionary Wedge" are shown in Figure 6.1 (SIS-16) and 6.2 (SIS-22). Profile SIS-16 (185 km in length) crosses the wedge approximately perpendicular to the deformation front, and parallel to the WSW tectonic transport direction, sampling roughly the frontal half of the potentially seismogenic fault plane (Figure 4.4). According to Thiebot and Gutscher (2006) the depth-migrated MCS profile images east dipping ramp thrusts soling out to a shallow east dipping decollement, as well as the eastward dipping sediment–basement interface (Figure 6.1.) As the frontal-most portion of an accretionary wedge is considered to deform aseismically (Byrne et al., 1988), it is likely that any co-seismic displacement may propagate along one of the prominent ramp thrusts. These ramp thrusts (sometimes called splay faults), typically have a dip of 30°–35° and are associated with 200–300 m scarps on the seafloor, which suggest fairly recent activity. The deeper portions of the accretionary wedge are less well imaged. The decollement can be followed to a maximum depth of 8–9 km (below sealevel), 30–50 km from the E end of the profile. The top basement interface is seen to be gently eastward dipping, parallel to the decollement, but cannot be imaged deeper than about 12 km depth (below sealevel). A dome-shaped feature is located at the deformation front (at the W end of profile) and disturbs the continuity of reflectors below. These may be anticlines related to thrust faulting or diapirs of unknown nature (mud volcanoes or salt diapirs).

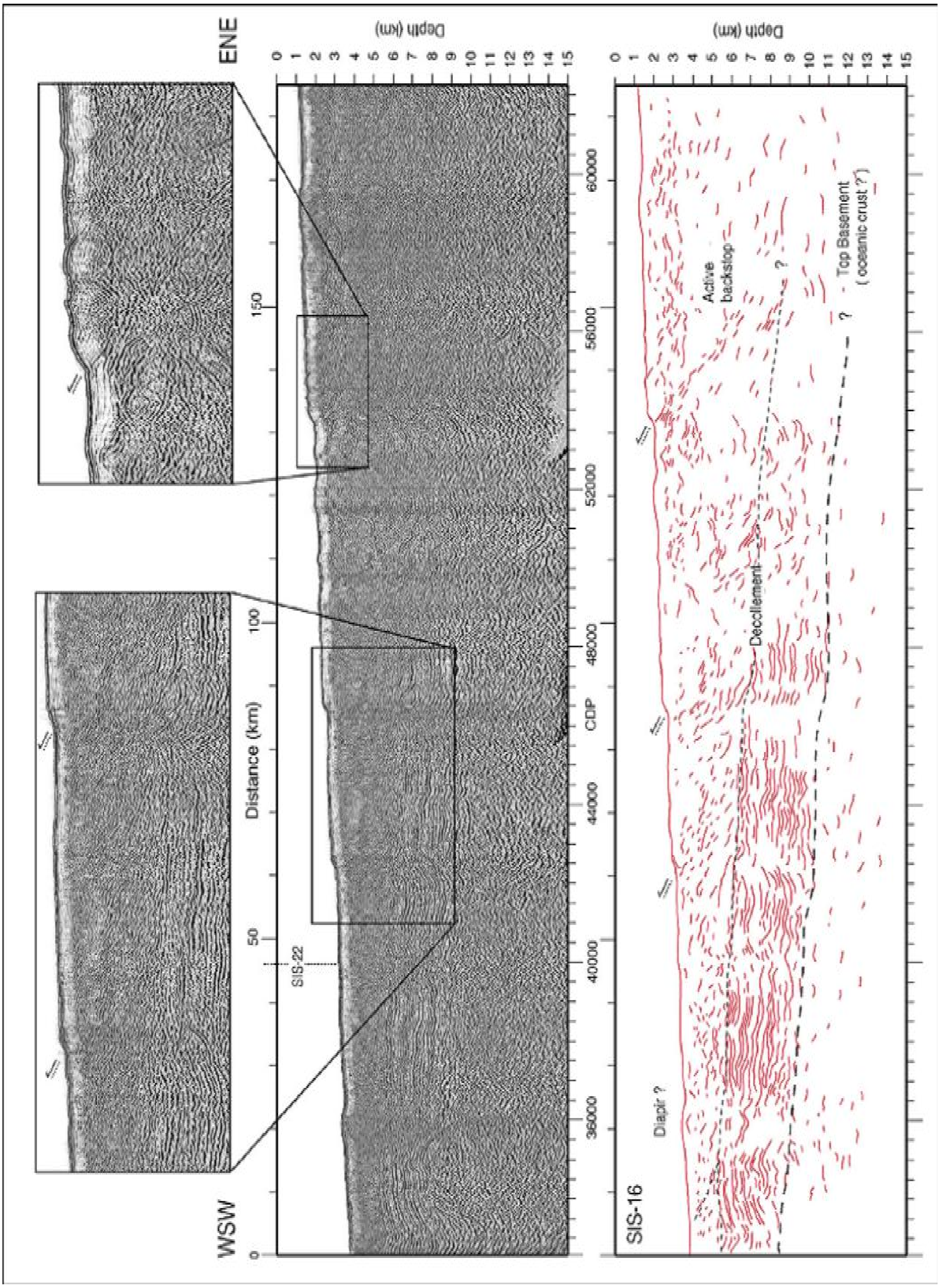

Figure 6.1.- *Multichannel seismic profile SIS-16, pre-stack depth migrated section. Central panel shows the entire 185 km long profile at a vertical exaggeration of 3:1. The lower panel is an interpreted line drawing (a depth cross-section). Upper panels show zooms of ramp thrusts emerging at the seafloor and the basal undeformed strata beneath the decollement. Thin dashed line is the decollement. Thick dashed line is top basement. Top continental basement has shorter dashing (from Thiebot and Gutscher, 2006).*

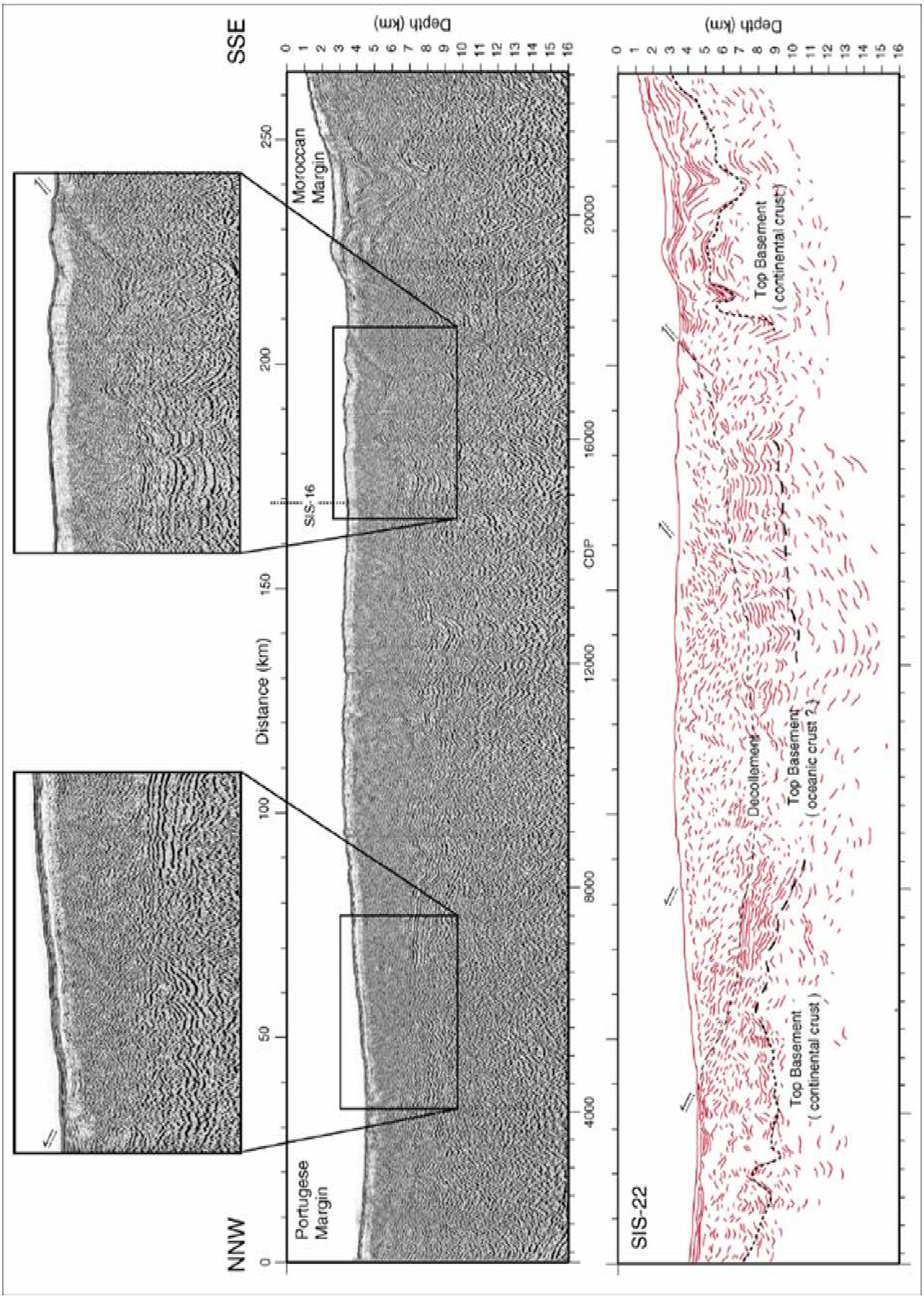

Figure 6.2.- *Multichannel seismic profile SIS-22, pre-stack depth migrated section. Central panel shows the entire 250 km long profile at a vertical exaggeration of 3:1. The lower panel is an interpreted line drawing (a depth cross-section). Upper panels show zooms of ramp thrusts at the deformation front, with the 2 s (TWT) thick basal series below the decollement. Dashed lines are the same as in Figure 6.1. (from Thiebot and Gutscher, 2006).*

SIS-22 is 265 km long, and crosses the accretionary wedge in a NNW–SSE direction, roughly perpendicular to the to the generally westward tectonic transport direction (Figure 6.2.) The dipping reflectors and thrust ramps at the N end of the profile (off the Portuguese margin) appear to be N vergent, and conversely, structures at the S end (off the Moroccan margin) appear to be S vergent. Thiebot and Gutscher (2006) suggest that these structures are in fact NW and SW vergent, respectively, along the lateral ramps of the westward vergent accretionary wedge. Profile SIS-22 images the same major crustal interfaces as profile SIS-16; dipping ramp thrusts soling out to a sub-horizontal decollement, and overlying a basal layer of undeformed sediments above the acoustic basement (Figure 6.2). The N and S portions of the profile image the Portuguese and Moroccan continental margins, respectively. Here the basement is known to be continental in nature, and the overlying sediments include carbonate platform strata of Mesozoic age. The basement beneath the accretionary wedge is likely to be a ~150 km-wide corridor of unknown nature. The central portion of the accretionary wedge is >7 km thick (4.5 km of deformed sediments above a 3 km thick basal layer).

In summary, the same pattern suggesting active subduction is claimed to be observed: undeformed horizontal basal reflectors, beneath a detachment horizon, seaward vergent (W, SW or NW) ramps intersecting the seafloor at a slope break between the horizontal abyssal plain, and the gentle ~1° undulating surface slope at the toe of the accretionary wedge (Figures 6.1 and 6.2).

6.2. The Horseshoe/Coral Patch Ridge faults (SW-02, SW-07, SW-13, AR-01)

The record sections corresponding to the profiles that cross the Horseshoe/Coral Patch Ridge faults are shown in Figure 6.3 (SW-13), 6.4 (SW-07), 6.5 (SW-02), and 6.6 (AR-01). These profiles have not been formally interpreted yet, so we just outline here the main structures that can be identified in the seismic sections. Its location is shown in Figure 4.5.

SW-13 extends for 205 km along the Horseshoe Abyssal Plain, the Coral Patch Ridge and the Seine Abyssal Plain with an NNW-SSE orientation. The most important structures crossed by the profile are the WNW-ESE Lineation S (corresponding to the bathymetric expression of the presently on-going dextral wrenching reactivation of WNW-ESE pre-existing faults) at CDP # 12300; the expression in depth of the Coral Patch Fault at CDP # 11700, a deep thrust cuitting the Jurassic basement (below 6 km depth) dipping southeast. According to our preliminary interpretation, this is a major structure accommodating the most of plate convergence along this line. The line also crosses the Coral Patch Ridge, which composed of a series of positive relieves generated by a series of narrowly conjugated spaced ENE-WSW trending folds and thrusts mainly with NW vergence that disrupt the sediments up to the basement. The Jurassic basement clearly shows numerous half-grabens that are result of the Triassic until Late Cretaceous North Atlantic spreading. Finally it crosses the Seine Abyssal Hills generated by NE-SW trending folds, also related to SE plate convergence, which locally get into the basement (Gràcia et al. 2003b) (Figure 6.3).

SW-07 (Figure 6.4) profile is 150 km-long and extends with an NNE-SSW orientation, from the southern part of the Marques de Pombal fault, through the Horseshoe Abyssal Plain and the Coral Patch Ridge and ends at the Seine Abyssal Plain. The profile crosses the southernmost expression of the Horseshoe fault at CDP # 4400. In this place the seafloor expression of the fault is a step of ~80 m only. It is not clear from this profile the depth that reaches this fault, but this could be partly due to its oblique orientation. The profile is also oblique to the Coral Patch ridge at CDP # 6800, showing disrupted sediments up to the top of the basement at 5800 m deep. The surface step associated to this fault is ~150 m.

Line SW-02 is one of the longest lines of the SWIM cruise (224 km; NW-SE), and crosses the Accretionary Wedge approximately perpendicular to the deformation front, obliquely to the South Lineation, perpendicular to the Horseshoe Fault and displays along the Horseshoe Abyssal Plain until the Gorringe Bank (Figure 6.5). The line is approximately perpendicular to the Horseshoe fault at CDP # 11100. This is one of the clearest depth images of this fault, clearly imaged as a reverse fault cutting the sediments and the basement to a depth of at least 9-10 km, which is the maximum depth reached with the system used in the cruise. Its seafloor expression is a step of ~160 m.

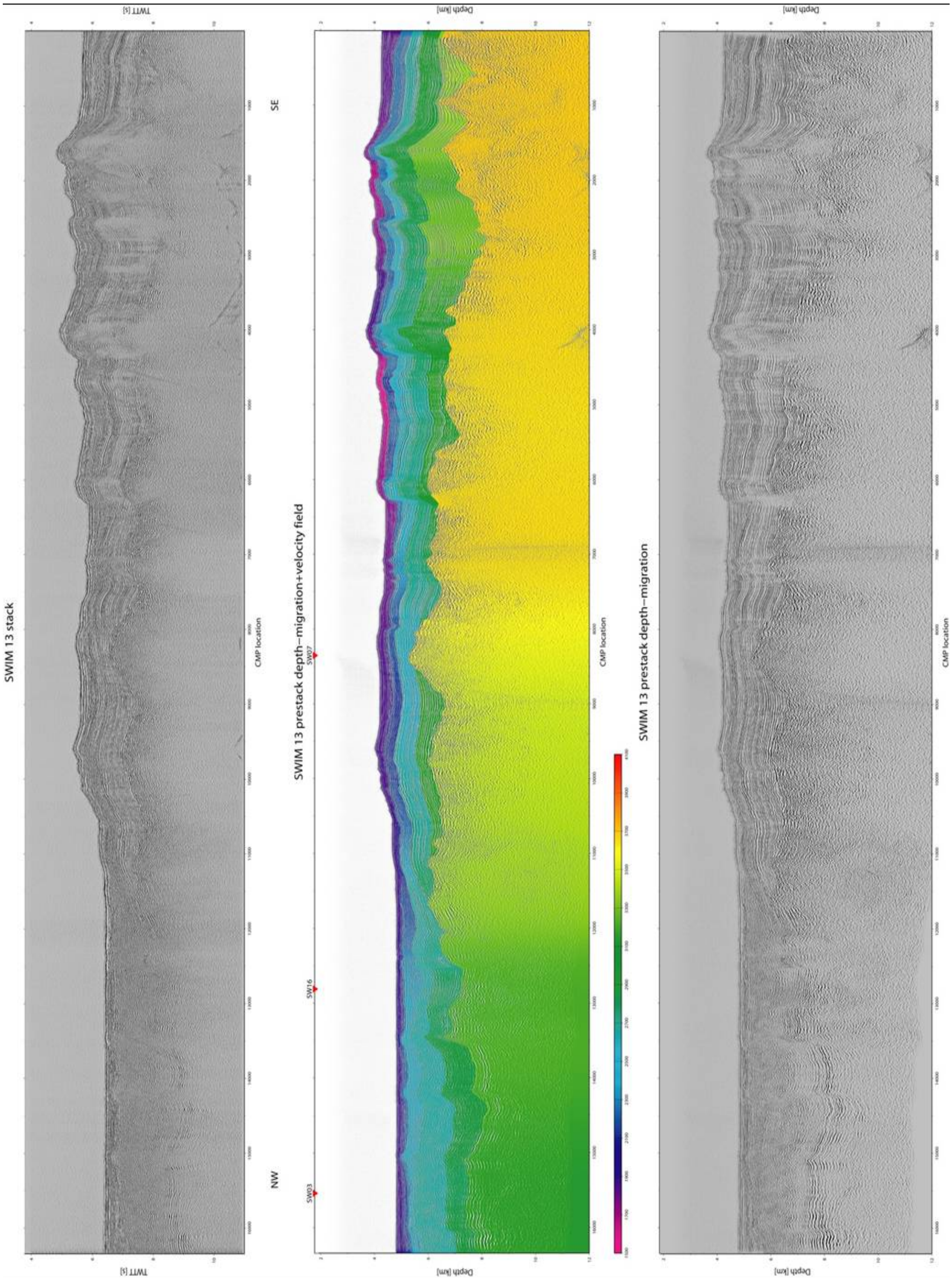

Figure 6.3.- *Multichannel seismic profile SW-13. Left panel is a stacked time-section, the central one is the PSDM section with the velocity model superimposed, the right one is the pre-stack depth migrated section. Red triangles indicate location of the SWIM-2006 MCS profiles that cross this line.*

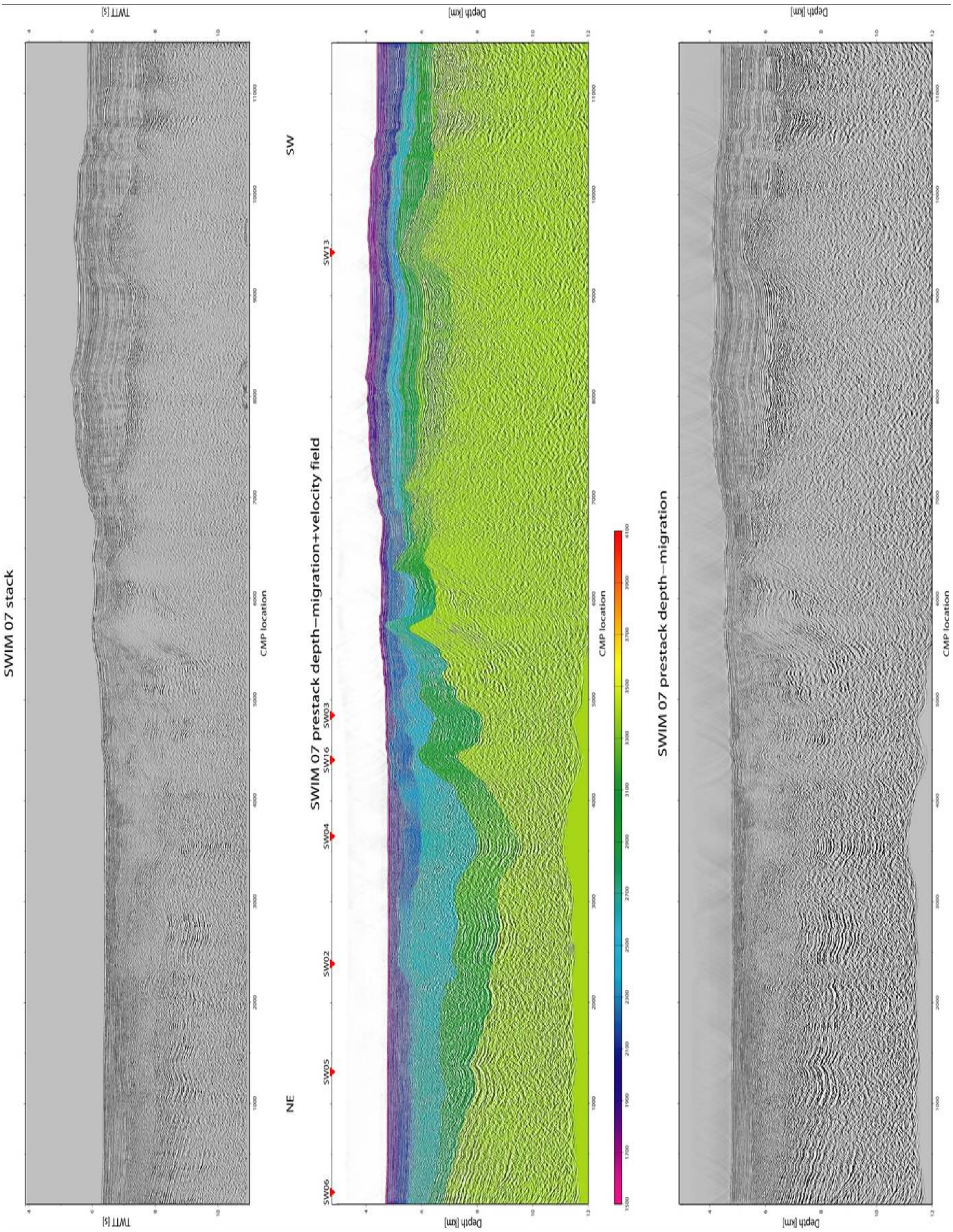

Figure 6.4.- *Multichannel seismic profile SW-07. Left panel is a stacked time-section, the central one is the PSDM section with the velocity model superimposed, the right one is the pre-stack depth migrated section. Red triangles indicate location of the SWIM-2006 MCS profiles that cross this line.*

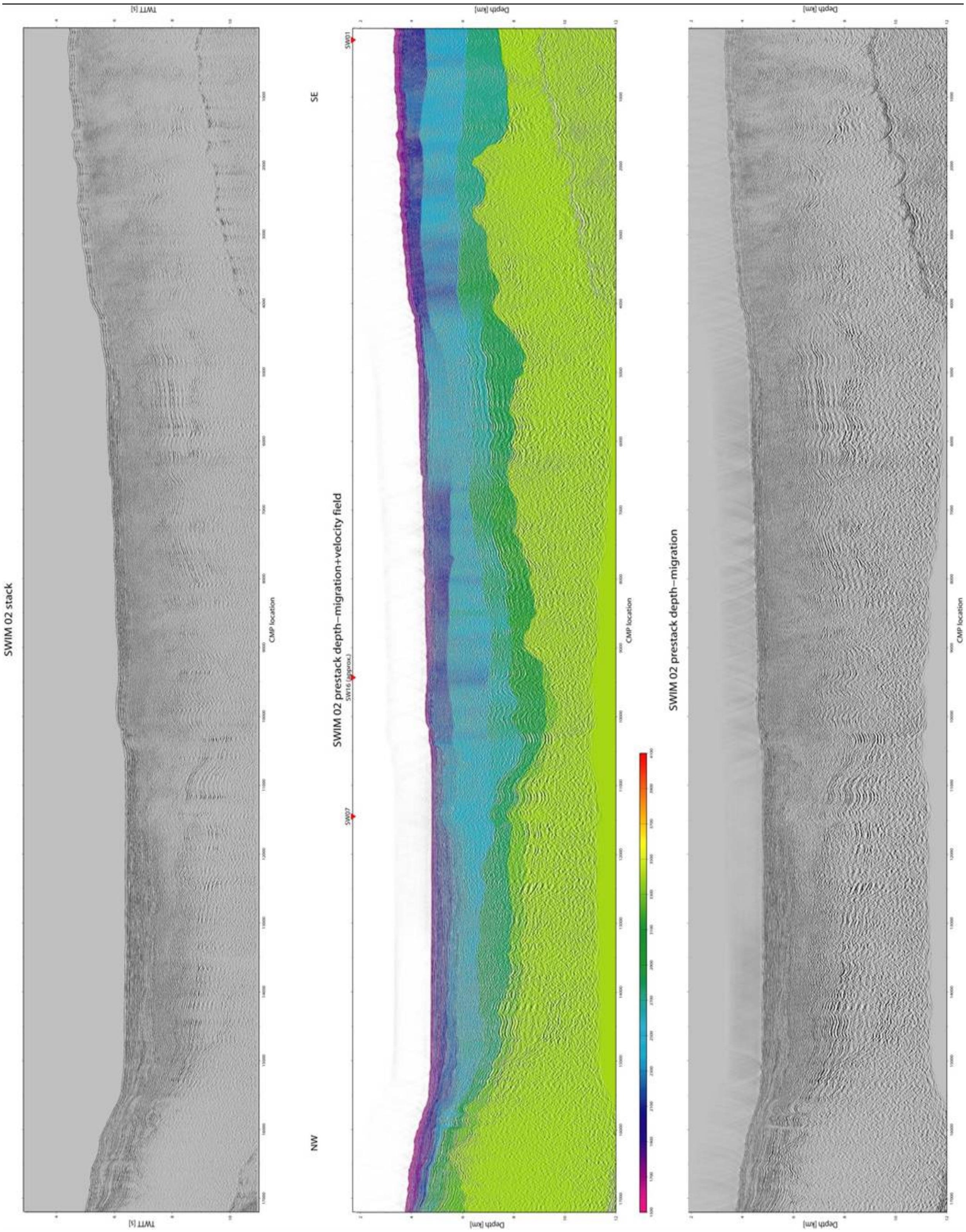

Figure 6.5.- *Multichannel seismic profile SW-02. Left panel is a stacked time-section, the central one is the PSDM section with the velocity model superimposed, the right one is the pre-stack depth migrated section. Red triangles indicate location of the SWIM-2006 MCS profiles that cross this line.*

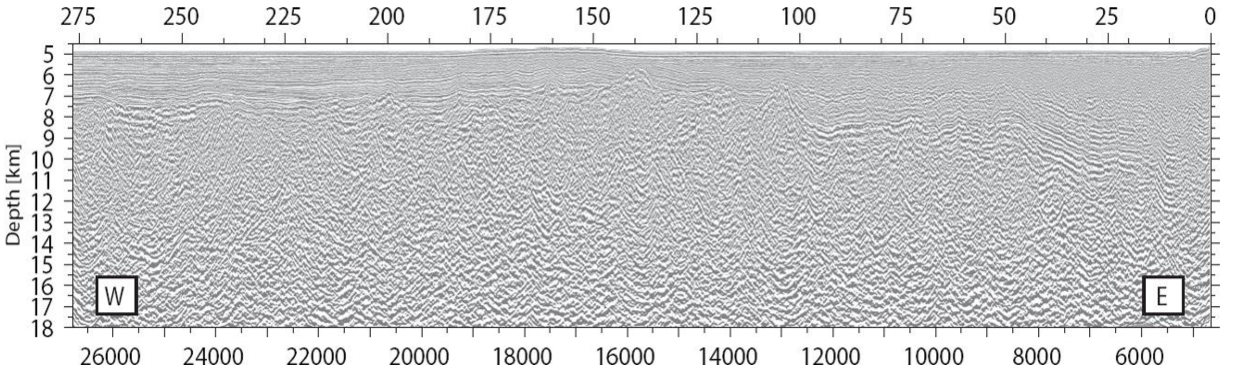

Figure 6.6.- *Easternmost section of the pre-stack depth migrated line along profile AR-01.*

6.3. The Gorringe Bank (IAM-4)

IAM-4 starts at the Coral Patch Ridge, crosses the Horseshoe Abyssal Plain and the Gorringe Bank and ends well within the Tagus Abyssal Plain. Its location is displayed in Figure 4.3. It is 386 km long and has a NW-SE orientation. This domain is characterised by a series of ridges and seamounts, which from North to South are: the Gorringe Bank and the Coral Patch and Ampere Seamounts. These regional SW-NE to WSW-ENE trending structures were uplifted after early Eocene times as a consequence of the convergence processes which may have started during the late Cretaceous (Olivet et al., 1984). The main structure crossed by this profile, and the most relevant for the section is thus the Gorringe Bank. Its basement made up of gabbros and metamorphosed basalts as suggested by DSDP site 120 results and it is interpreted as a large tilted block of oceanic nature and ultrabasic composition (Ryan et al., 1973) that overthrusts the Tagus Abyssal Plain for 4-5 km at least, and shows a strikingly different degree of tectonic deformation to NW and SE.

The corresponding seismic image (Figure 6.7) does not shed much light on the deep structure of the bank. The high velocities needed for migration are consistent with the inferred mantle-like composition of the bulk rock that constitutes the block, but the presence of numerous, chaotic multiples make difficult to get a correct, interpretable image of the sub-seafloor, especially beneath the crest of the ridge. Also there are not clear faults penetrating deep into the basement.

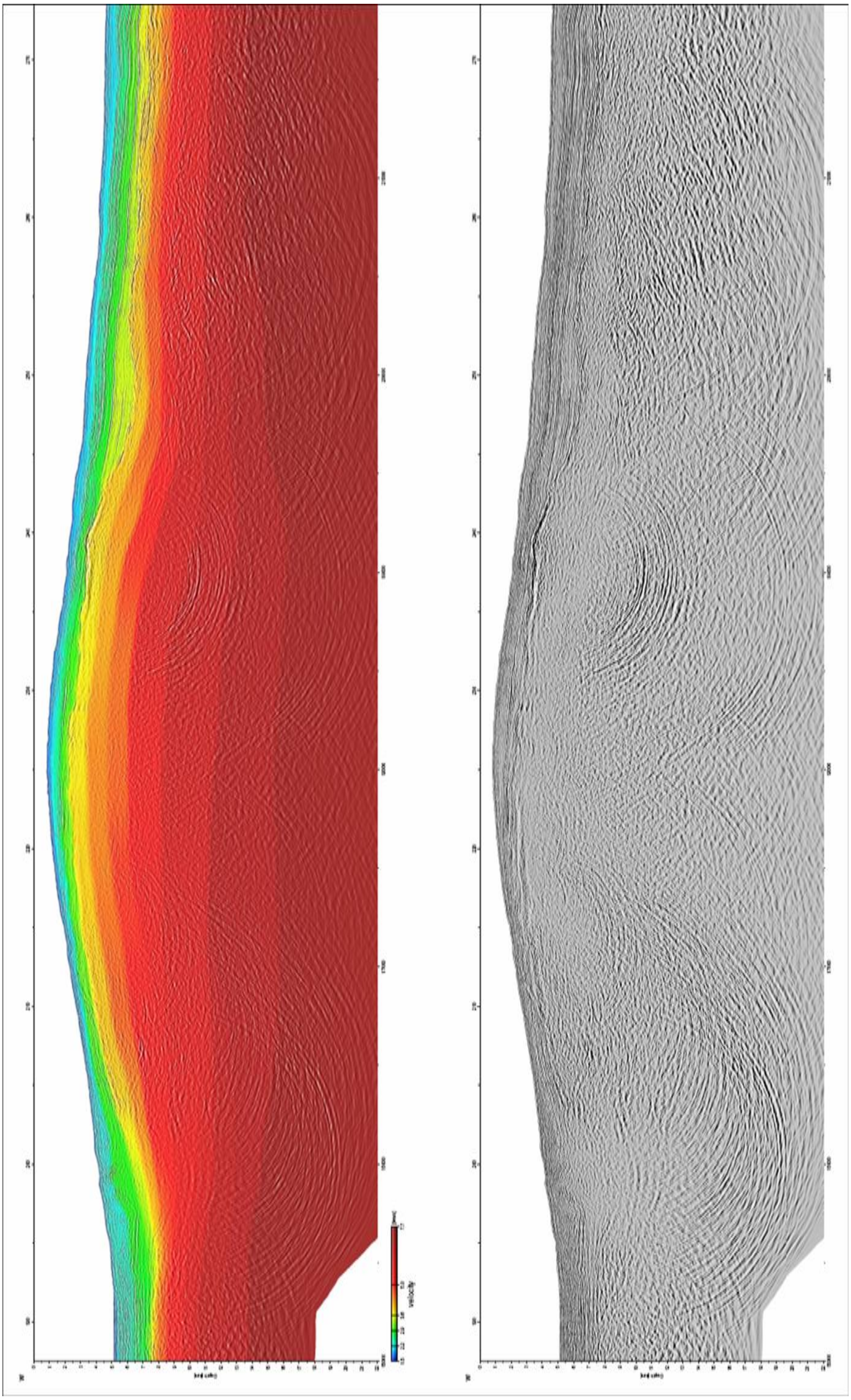

Figure 6.7.- *Detail of the northern section of multichannel seismic profile IAM-4 crossing the Gorringe bank. Left panel is is the PSDM section with the velocity model superimposed, whereas the right one is the pre-stack depth migrated section.*

6.4. The Marques de Pombal fault system (AR-10)

Line AR-10 runs with a NNW-SSE orientation and is the closer to the SW Iberian coast (see Figure 4.2 for location). The profile reveals a prominent thrust structure associated with evidence of ongoning tectonic deformation (at the south part of the profile) with intense folding, disruption of stratigraphic units and uplift of the seafloor. The deformed area encompasses the whole line (about 200 km in length) and the thrust structure alone can be followed for more than 50 km. In Figure 6.8 we show a detail of the part of the profile crossing the main Marques de Pombal fault zone. Northwestward of the major thrust plane the sedimentation has been continuous furnishing the complete record of syn-compressional sediments above the pre-compressional sediments. In places, the seafloor morphology is slightly controlled by folding. Between 5 to 25 km (Figure 6.8) the thrust structure is decoupled by a deep décollement surface, recognizable down to 10 s TWT (about 12-15 km depth), with a dip-slip throw of more than 1100 m affecting the whole sedimentary cover and the basement. South-eastwards, the décollement surface seems shallower, about 9 s TWT, and is accompanied by folding with minor thrusting. Here the deformation, as inferred from the setting of the sedimentary cover, is still active with displacement of the seafloor (Zitellini et al., 1999).

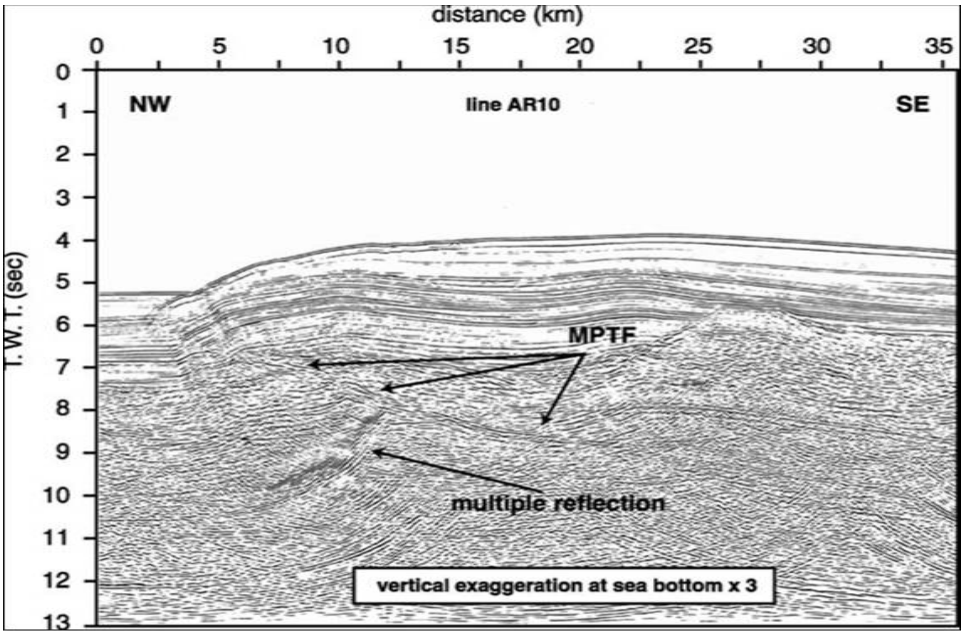

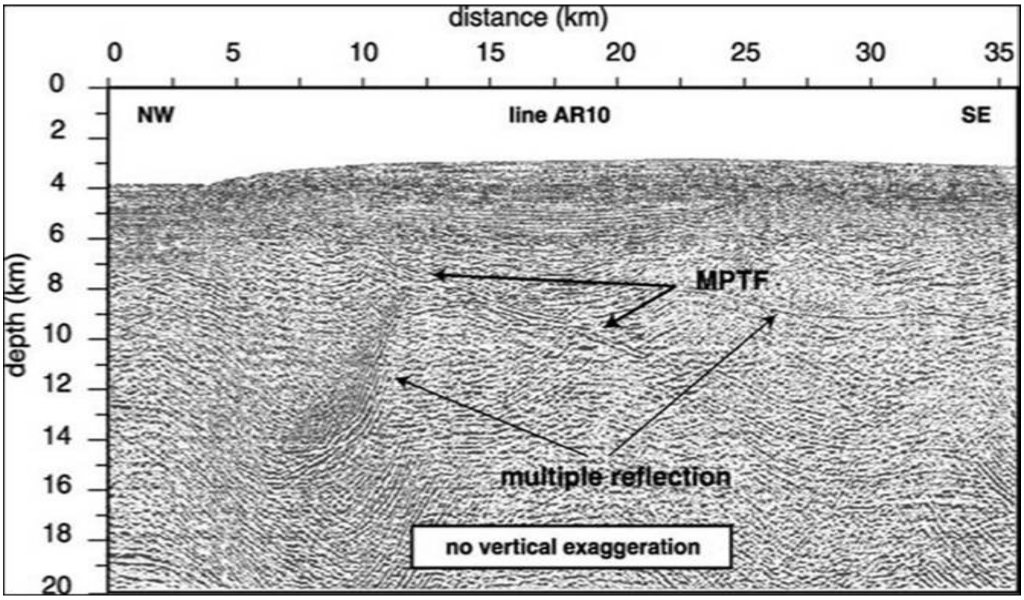

Figure 6.8.- *(previous page) Time migration of the part of profile AR-10 crossing the Marques de Pombal thrust area. (This page) PSDM section of the same part of the profile.*

6.5. The WNW-ESE fault lineations (SW-01, SW-16)

MCS data allows distinguishing different geometries from west to east along the lineations. The southern lineation (LS) doesn't reach up the surface in its western limit (Horseshoe Abyssal Plain) but seismic data reveal a flower-structure that doesn't affect the upper sediment layers. So, in the western part we have seismic evidences of strike-slip faulting to enlarge the LS further to the west where the bathymetry data don't reveal any topographic relief (Figure 6.9).

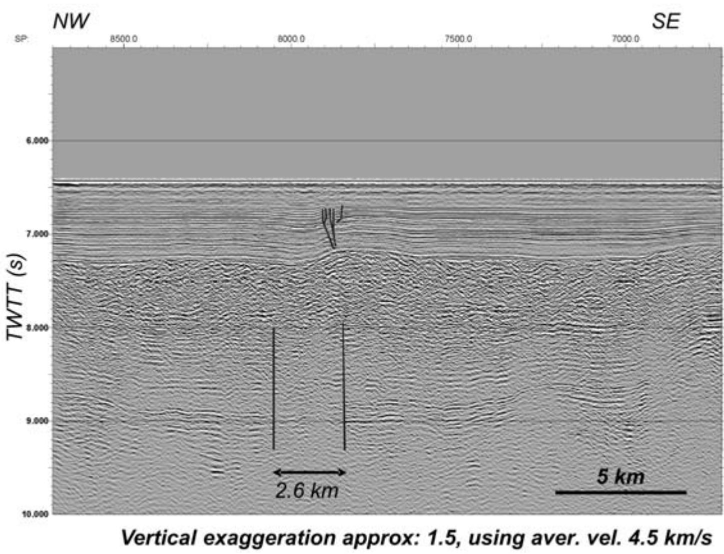

Figure 6.9.*- Zoom between CDP´s 6500-9000 of the time migration of the profile SW09, showing a flower-structure in the sediments that doesn't reach the surface. The "transparent" 2.6 km wide zone is the area affected by the strike-slip faulting, where the sediment structure is lost*

From the central to the eastern part of the LS the transference zone between the two blocks of the fault is well imaged by MCS data at least until 10 km depth. The active strike slip zone is ~6 km wide in profile SW16 (Figure 6.11), ~2 km in profile SW13 (Figure 6.3) and ~7 km in profile SW03. A detail of the transference zone for these profiles is shown in Figure 6.10. The wide range of these values reflects the obliquity of the orientation of the profile respect to the LS. The active area between the two blocks of the fault reaches at least 10 km depth, the maximum vertical penetration of the system. Recent estimations of depth and seismic moment tensors (M_w 3.8 to 5.3) from time domain inversion of near-regional waveforms show reverse and strike-slip faulting solutions between 6 and 60 km depth over the LS (Stich et al., 2005), consistent with our seismic observations.

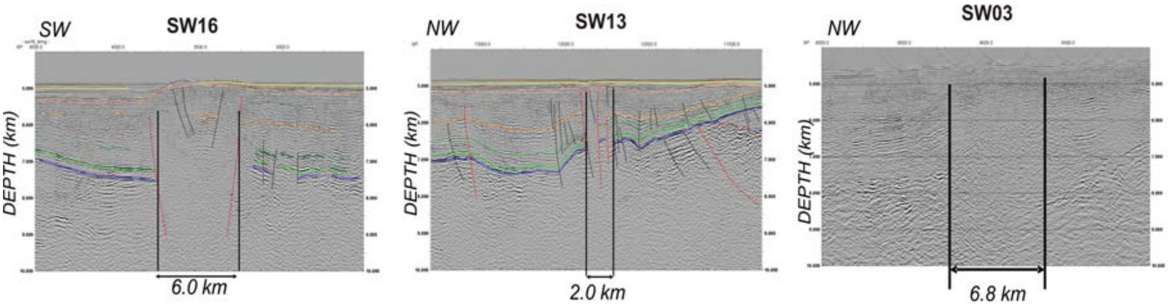

Figure 6.10.- *Zoom of the profiles SW16, SW13 and SW03 crossing obliquely the LS. The 6.0 km, 2.0km and 6.8 km wide "transparent" zone, illustrate the area where one block is moving against the other. The large range of the values depends on the different oblique angle of the profiles crossing the structure. Vertical exaggeration 2.5*

The analysis of the MCS data recorded along structure (e.g. profile SW01; Figure 6.12) indicates that the motion is dextral strike-slip and some vertical component is also observed. The surface evidence of pushing up forces in the fault area is a vertical relief of up to 80 m high reaching up to the surface. The active strike slip zone, crossed perpendicular by the profile, is 57 km long, ~8.7 km wide, and the basement shows a lateral step of over 2 km. Both lineations, match the compressional frame between Eurasia and Africa since their WNW-ESE orientation is consistent with the NW-SE convergence of the Gulf of Cadiz.

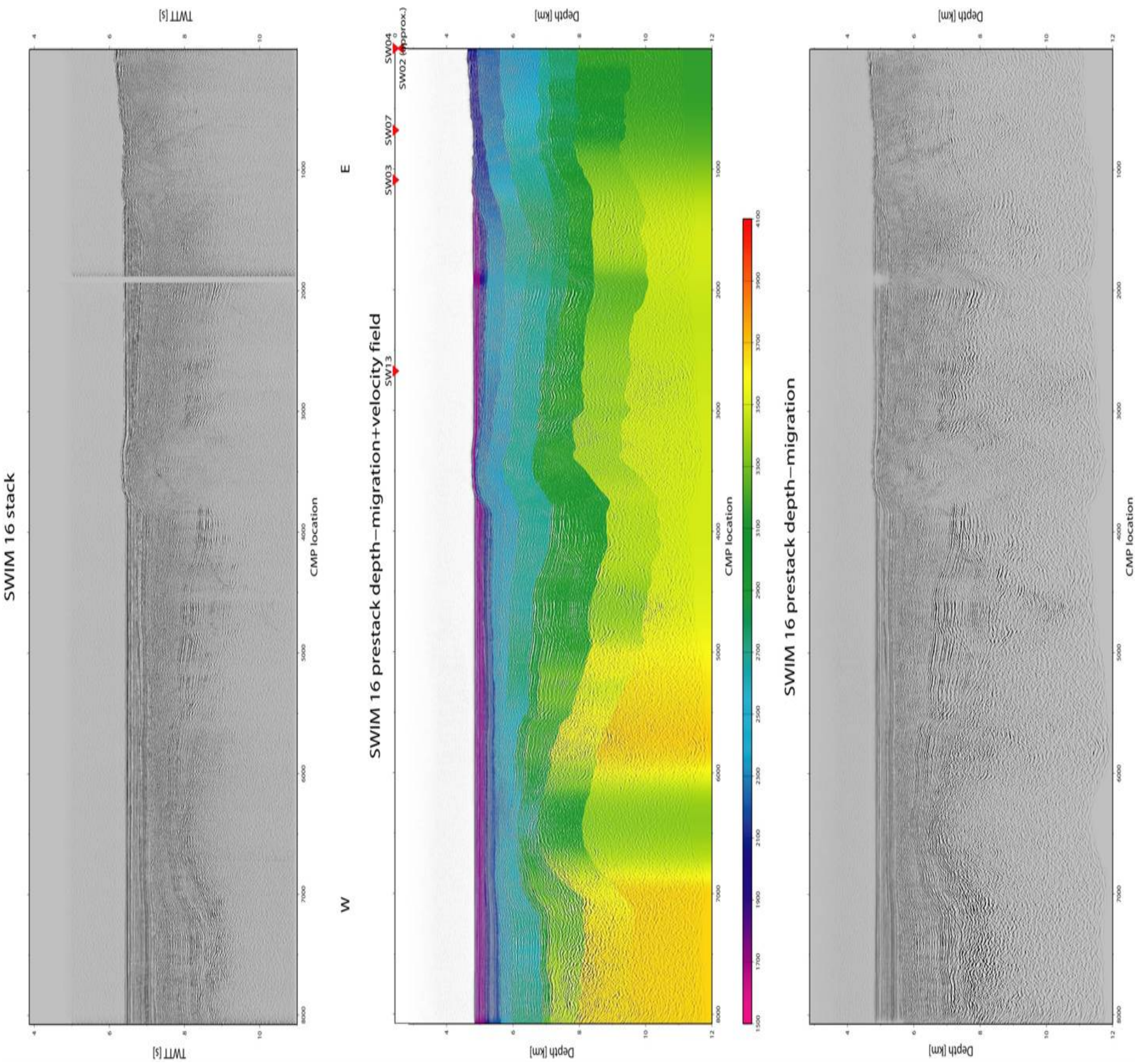

Figure 6.11.- *Multichannel seismic profile SW-16. Left panel is a stacked time-section, the central one is the PSDM section with the velocity model superimposed, the right one is the pre-stack depth migrated section. Red triangles indicate location of the SWIM-2006 MCS profiles that cross this line.*

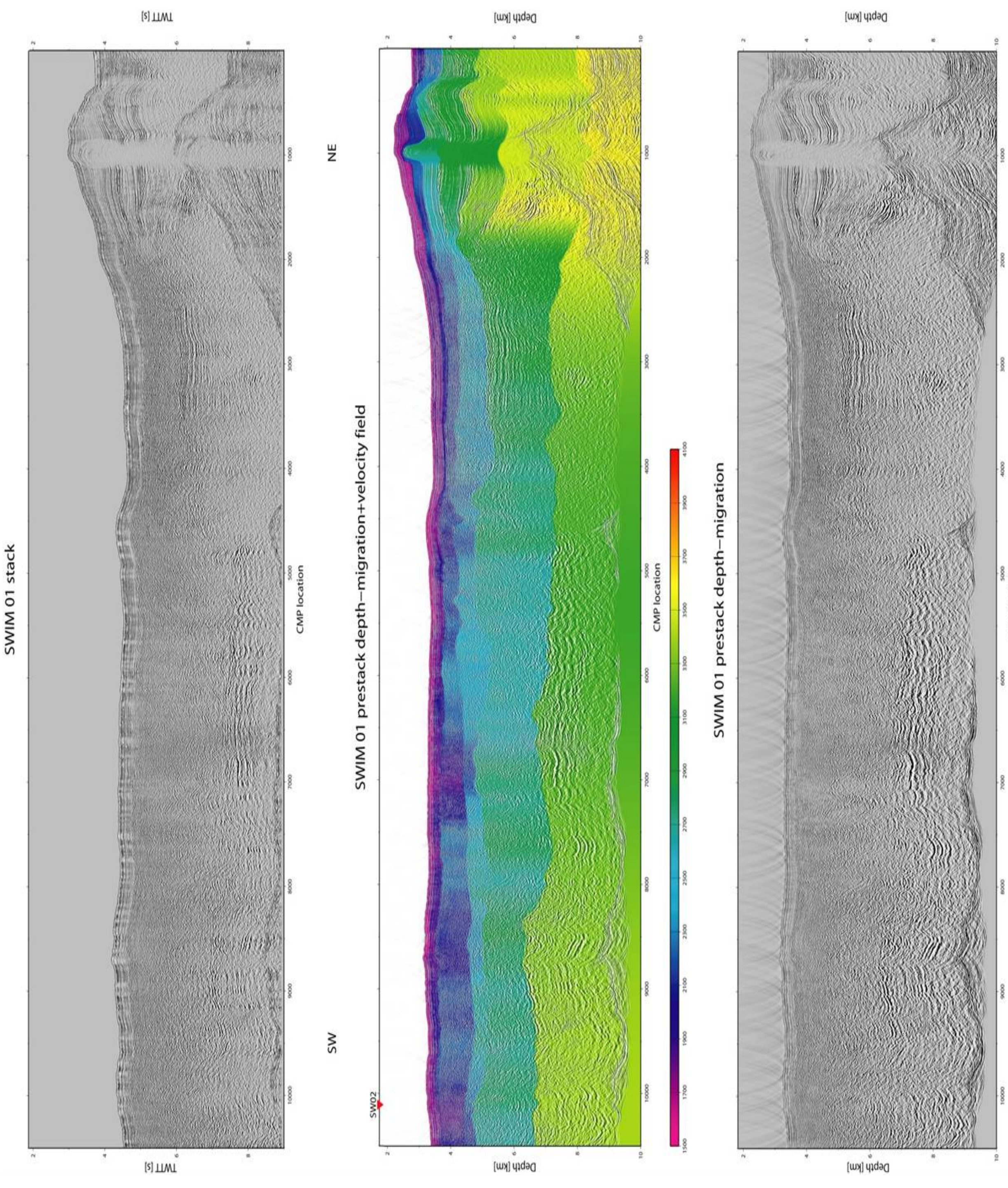

Figure 6.12.- *Multichannel seismic profile SW-01. Left panel is a stacked time-section, the central one is the PSDM section with the velocity model superimposed, the right one is the pre-stack depth migrated section. Red triangles indicate location of the SWIM-2006 MCS profiles that cross this line.*

7. Conclusions

The compilation of pre-stack depth migrated multi-channel seismic profiles in the Gulf of Cadiz, in combination with the previous review of the tectonic structures made by Terrinha et al. (2008), have allowed to better characterize the deep structure, geometry and functioning of the major faults that shape the different tectonic domains. The main conclusions for each domain are summarized next.

Accretionary Wedge: profiles SIS-16 and SIS-22 (Figures 6.1 and 6.2) show a rather consistent pattern of undeformed horizontal basal reflectors beneath a detachment horizon. We observe seaward vergent ramps intersecting the seafloor at a slope break between the horizontal abyssal plain, and a gentle dipping undulating surface at the toe of the wedge, but deeper the image is poorer. Active subduction beneath the wedge is an attractive hypothesis that is compatible with these observations, so this candidate can not be discarded based on MCS alone. However MCS does not provide compelling evidences of active subduction and other processes could also explain the observations.

Horseshoe/Coral Patch Ridge faults: The Horseshoe fault is clearly imaged by the perpendicular SW-02 profile (Figure 6.5). This reverse fault shows a prominent seafloor escarpment and sharply disrupts the basement up to a depth of at least 9-10 km. It is also the source of significant recent seismicity and seismological modelling indicates that it is a likely source for large earthquakes. MCS strongly supports this hypothesis, especially in what refers to its northern segment. The fault is less well imaged to the south by profile SW-0. There its surface expression is smaller its depth reach is undefined (Figure 6.4). The Coral Patch Ridge fault is imaged in profile SW-13 as a major, SE dipping, thrust fault cutting deep into the basement that may have accommodated to date most plate convergence in this segment and be a likely source of large earthquakes (Figure 6.3). Conversely, the Coral Patch Ridge and the SE thrust-and-fold system are imaged as a series of reverse faults linked to plate convergence that do not affect the basement.

Gorringe Bank: IAM-4 profile cuts this prominent structure that is believed to thrust the Tagus Abyssal plain for 4-5 km at least. However the corresponding seismic image (Figure 6.7) is masked by numerous chaotic multiples making impossible to get a clear, interpretable image of the sub-seafloor, especially beneath the crest of the ridge. The high velocities needed for migration are consistent with the inferred bulk mantle-like composition of the block, but no clear faults penetrating deep into the basement can be identified in the seismic image. In summary, MCS does not help resolving the deep structure of this feature, and the acquisition complementary (wide-angle) seismic data is strongly recommended to shed some light into its deep structure.

Marques de Pombal fault system: Profile AR-10 (Figure 6.8) shows a spectacular thrust structure associated to the fault with evidence of ongoning tectonic deformation. The thrust structure alone can be followed for more than 50 km as a bright, continuous deep décollement surface that reaches a depth of 12-15 km at least. The deformation is still active with displacement of the seafloor. AR-10 provides therefore a strong evidence for the presence of a major, deeply-rooted, currently active structure that could well be the source of large earthquakes. Although its size is too small to generate an Mw 8.5-8.7 earthquake, the combination of this fault with some of its neighbours (e.g. Horseshoe fault) is an option that deserves being carefully analyzed.

WNW-ESE fault lineations: The southern lineation is cut by a number of SWIM-06 profiles at various sectors, e.g., SW16, SW13, SW03 (e.g. Figure 6.10), which show that this active strike-slip fault is deforming the basement up to more than 9-10 km. The sediments are affected by a morphologic flower-structure, characteristic of a strike-slip faulting. The fault can be followed deeper up to well inside the Horseshoe Abyssal Plain. Profile SW-01 (Figure 6.12) provides an excellent image of the northern lineation, whose basement shows an outstanding vertical displacement of over 2 km. They are not likely sources of the largest regional earthquakes, but based on their dimensions they may generate earthquakes of Mw up to 7.5. None of these lineations seem to be a reliable tsunami source. Both lineations match the regional NW-SE compressional regime, so they could well play a key role in accommodating the present-day Africa-Eurasia convergence in the region.

8. Acknowledgements

We acknowledge the PIs of projects AR-RIFANO-1992, IAM-1994, SISMAR-2001, and SWIM-2006, for providing the data and/or depth migrated sections that are included in this report. Also, we thank the different contributors of the deliverable, and especially Rafael Bartolomé, and Sara Martínez for their effort during these last days. Also thanks to Gabriela Carrara for finding the time to send us the Rifano profiles, to Marc-André Gutscher for providing us with the SISMAR ones, and to the rest of Nearest-WP2 contributors for their support. Special thanks to Luis Pinheiro, who provided us with the PSDM-migrated IAM-4 profile. Any reference to this profile should be consulted with him. Also thanks to Pedro Terrinha, whose tectonic compilation has been used as a base for this work. Finally, a big hug and our best wishes to our friend Eulàlia Gràcia, CSIC's team leader who is now getting over of a bad experience at home. We really missed her advice with the final writing of this report!

9. References

Abe, K., 1989. Size of great earthquakes of 1837-1974 inferred from tsunami data. *J. Geophys. Res*. 84, 1561-1568.

Auzende, J.M., Olivet, J., Charvet, J., Le Lann, A., Le Pichon, X., Monteiro, J., Nicolas, A. and Ribeiro, A., 1978. Sampling and observation of oceanic mantle and crust on Gorringe Bank. *Nature* 273: 45–48.

Auzende, J. M. et al. (group CYAGOR II). 1982. The Gorringe Bank: First Results of Submersible Expedition CYAGOR II, *Terra Cognita* 2, 123-130.

Banda, E., Torné, M., 1995. Iberian Atlantic Margins Group investigates deep structure of ocean margins, *Eos Trans. AGU* 25.

Baptista, M.A., Heitor, S., Miranda, J.M., Miranda, P.M.A., Mendes Victor, L., 1998a. The 1755 Lisbon; evaluation of the tsunami parameters. *J. Geodyn*. 25, 143–157.

Baptista, M.A., Miranda, P.M.A., Miranda, J.M., Mendes Victor, L., 1998b. Constraints on the source of the 1755 Lisbon tsunami inferred from numerical modelling of historical data on the source of the 1755 Lisbon tsunami. J. Geodyn. 25, 159–174.

Bartolomé, R., Contrucci, I., Neuze, H., Thiebot, E. & Klingelhoefer, F., 2004. Improving the "single bubble" multi-channel vertical seismic image with pre-stacik depth migration by using the OBS wide-angle reflection/refraction velocities: example of the Moroccan margin. *J. Appl. Geophys*. 57 (2), 107–118.

Bartolome, R., Gràcia, E., D. Stich, D., D. Klaeschen, D., Martínez, S., Terrinha, P., Dañobeitia, J.J., Zitellini, N., SWIM Working Group. 2008 . Seismic evidence of active strikeslip faulting in the Horseshoe Abyssal Plain (SW Iberian Margin). European Geosciences Union (*EGU*)-08, Vienna (Austria), 13-18 April

Buforn, E., Udias, A., Colombas, A., 1988. Seismicity, source mechanisms and tectonics of the Azores–Gibraltar plate boundary. *Tectonophysics* 356, 89–118.

Byrne, D.E., Davis, D.M., Sykes, L.R. 1988. Loci and maximum size of thrust earthquakes and the mechanics of the shallow region of subduction zones. *Tectonics*. 7: 833–857.

Contrucci, I., Klingelhofer, F., Perrot, J., Bartolome, R., Gutscher, M.-A., Sahabi, M., Re´hault, J.-P., Malod, J., 2004. The crustal structure of the NW Moroccan continental margin from wideangle and reflection seismic data. *Geophy. J. Int*. 159 (1), 117– 128.

Dañobeitia, J. J., Bartolomé, R., Checa, A., Maldonado, A., and Slootweg, A. P. 1999. An interpretation of a prominent magnetic anomaly near the boundary between the Eurasian and African plates (Gulf of Cadiz, SW margin of Iberia), *Mar. Geol*., 155, 45 – 62.

Diez, S.; Gràcia, E.; Gutscher, M.A.; Matias, L.; Mulder, T.; Terrinha, P.; Somoza, L.; Zitellini, N.; De Alteriis, G.; Henriet, J.P.; Dañobeitia, J.J. 2005. Bathymetric map of the Gulf of Cadiz, NE Atlantic Ocean: The SWIM multibeam compilation. *250th Anniversary of the 1755 Lisbon Earthquake*, Lisbon (Portugal), 1-4 November.

Féraud, G., York, D., Mevel, C., Cornen, G., Hall, C.M., and Auzende, J.M. (1986). Additional 40Ar/39Ar dating of the basement and the alkaline volcanism of Gorringe Bank (Atlantic Ocean). *Earth Planet*. Sci. Lett. 79: 255–269.

Fukao, Y., 1973. Thrust faulting at a lithospheric plate boundary: the Portugal earthquake of 1969. *Earth Planet. Sci*. Lett. 18, 205–216.

Galindo-Zaldívar, J., Gil, A.J., Borque, M.J., González-Lodeiro, F., Marín-Lechado, C., Jabaloy, A., Ruano, P., Sanz de Galdeano, C. 2003. Active faulting in the internal zones of the central Betic Cordillera (SE Spain). *J Geodynam* 36:239–250

Girardeau, J., Cornen, G., Beslier, M.O., Le Gall, B., Monnier, C., Agrinier, P., Dubuisson, G., Pinheiro, L., Ribeiro, A., and Whitechurch, H. 1998. Extensional tectonics in the Gorringe Bank rocks, Eastern Atlantic Ocean: evidence of an oceanic ultra-slow mantellic accreting center, *Terra Nova*. 10: 330–336.

Gonzalez-Fernandez, A., Cordoba, D., Matias, L., Torne, M., 2001. Seismic crustal structure in the Gulf of Cadiz (SW Iberian Peninsula). *Mar. Geophys. Res*. 22, 207–223.

Gràcia, E., Dañobeitia, J.J., Vergés, J., Team, P., 2003a. Mapping active faults offshore Portugal (36°N-38°N): implications for seismic hazard assessment in the SW Iberian Margin. *Geology*. 31, 83–86.

Gràcia, E., Doñabeitia, J., Vergés, J., Bartolomé, R., Córdoba, D., 2003b. Crustal architecture and tectonic evolution of the Gulf of Cadiz (SW Iberian margin) at the convergence of the Eurasian and African plates. *Tectonics*. 22. doi:10.1029/2001TC901045, 2003.

Gràcia, E. et al., 2008. Nearest Project, Deliverable D2: Review of Sources due to Slope Inestabilities.

Grimison, N.L., W.P. Chen. 1986. The Azores-Gibraltar plate boundary: Focal mechanisms, depths of earthquakes and their tectonic implications. *J. Geophys. Res*. 91, 2029-2047.

Gutscher, M.-A., Malod, J., Rehault, J.-P., Contrucci, I., Klingelhoefer, F., Mendes-Victor, L., Spakman, W., 2002. Evidence for active subduction beneath Gibraltar. *Geology* 30, 1071–1074.

Hayward, N., Watts, A.B., Westbrook, G.K., Collier, J.S., 1999. A seismic reflection and GLORIA study of compressional deformation in the Gorringe Bank region, eastern North Atlantic. *Geophys. J. Int*. 138, 831–850.

Iribarren, L., Vergés, J., Camurri, F., Fullea, J., Fernàndez, M., 2007. The structure of the Atlantic-Mediterranean transition zone from the Alboran Sea to the Horseshoe Abyssal Plain (Iberia–Africa plate boundary). *Mar. Geol.*, 243, 97-119.

Kazmin et al. 1990

Maldonado, A., Somoza, L., Pallarés, L., 1999. The Betic orogen and the Iberian–African boundary in the Gulf of Cadiz: geological evolution (central North Atlantic). *Mar. Geol.* 155, 9–43.

McBarnet, A., 2000. How GXT caught the pre-stack depth imaging wave, First Break 18 (3), 109–111.

Medialdea, T., Vegas, R., Somoza, L., Vázquez, J.T., Maldonado, A., Díaz-del-Rio, V., Maestro, A., Córdoba, D., Fernández-Puga, M.C., 2004. Structure and evolution of the “Olistostrome” complex of the GibraltarArc in theGulf ofCadiz (eastern CentralAtlantic): evidence from two long seismic cross-sections. *Mar. Geol.* 209, 173–198.

Mendes Victor et al. 1990

Mendes Victor, L., Baptista, M.A., Miranda, J.M., Miranda, P.M.A., 1999. Can hydrodynamic modelling of tsunami contribute to seismic risk assessment? *Phys. Chem. Earth* 24, 139–144.

Olivet, J.L., Bonnin, J., Beuzart, P., and Auzende, J.M., 1984. Cinématique de l’Atlantique nord et central. Cent. Natl. Exploit. Oceans, Peris. *Rapp. Sci. Tech*. 54, 108.

Rovere, M., Ranero, C.R., Sartori, R., Torelli, L., Zitellini, N., 2004. Seismic images and magnetic signature of the Late Jurassic to Early Cretaceous Africa–Eurasia plate boundary off SW Iberia. *Geophys. J. Int*. 158, 554–568.

Roque et al 2007

Ryan, W.B.F., et al., 1973. Initial Reports of the Deep Sea Drilling Project. U.S. Government Printing Office,Washington, D.C., p. 514.

Sandwell, D. T., and W. H. F. Smith. 1997. Gravity anomaly from Geosat and ERS1 satellite altimetry, J. Geophys. Res., 102, 10,039 – 10,054.

Sartori, R., Torelli, L., Zitellini, N., Pevis, D., and Lodolo, E., 1994. Eastern segment of the Azores-Gibraltar line (central-eastern Atlantic): An oceanic plate boundary with diffuse compressional deformation, *Geology* 22: 555–558.

Somoza, L., V. Díaz-del-Río, R. León, M. Ivanov, M. C. Fernández-Puga, J. M. Gardner , F. J. Hernández-Molina, L. M. Pinheiro, J. Rodero, A. Lobato, et al., 2003. Seabed morphology and hydrocarbon seepage in the Gulf of Cádiz mud volcano area: Acoustic imagery, multibeam and ultra-high resolution seismic data. *Marine Geology*, 195, Issues 1-4, 30 Pages 153-176.

Stich, D., Mancilla, F., Morales, J., 2005. Crust mantle coupling in the Gulf of Cadiz (SW Iberia). *Geophys. Res. Lett.*, 32, L13306, doi: 10.1029/2005GL023098.

Stich, D., Mancilla, F., Pondrelli, S., Morales, J., 2007. Source analysis of teh February 12th 2007, Mw 6.0. Horseshoe earthquake: Implications for the 1755 Lisbon earthquake. *Geophys. Res. Lett*., 34, L11208, doi: 10.1029/2007GL030012.

Stirling, M., Rhoades, D., and Berryman, K., Comparison of earthquake scaling relations derived from data of the instrumental and preinstrumental era, *Bull. Seism. Soc. Am.,* Vol. 92, Nº2, pp. 812-830, 2002.

Terrinha, P., 1998. Structural geology and tectonic evolution of the Algarve Basin, South Portugal. *PhD Thesis, Imperial College*, London, 400 pp.

Terrinha, P., Pinheiro, L.M., Henriet, J.P., Matias, L., Ivanov, M.K., Monteiro, J.H., Akhmetzhanov, A., Volkonskaya, A., Cunha, T., Shaskin, P. & Rovere, M. 2003. Tsunamigenic-seismogenic structures, neotectonics, sedimentary processes and slope instability on the southwest Portuguese Margin. *Mar. Geol*. 195(1-4), 55-73.

Terrinha, P., Valadares, V., Duarte, J., Roque, C., Duarte, H., Vicente, J., Rosas, F., and Matias, L. 2008. Nearest Project, Deliverable D1: Review of tectonic Sources.

Thiebot, E., Gutscher, M.-A., 2006. The Gibraltar Arc seismogenic zone (part 1): constraints on a shallow east dipping fault plane source for the 1755 Lisbon earthquake provided by seismic data, gravity and thermal modeling. *Tectonophysics* 246, 135–152.

Torelli, L., Sartori, R., Zitellini, N., 1997. The giant chaotic body in the Atlantic Ocean off Gibraltar: new results from a deep seismic reflection survey. *Mar. Pet. Geol.* 14, 125–138.

Tortella, D., Torné, M., Pérez-Estaún, A., 1997. Geodynamic Evolution of the Eastern Segment of the Azores–Gibraltar Zone: the Gorringe Bank and the Gulf of Cadiz Region. *Mar. Geophys. Res*. 19, 211–230.

Wells, D., and K. Coppersmith, New empirical relationships among magnitude, rupture length, rupture width, rupture area, and surface displacement, *Bull. Seism. Soc. Am.,* Vol. 84**,** 974–1002, 1994.

Yilmaz, O., 1987. Seismic Data Processing. *Society of Exploration Geophysics*, Tulsa.

Zitellini, N., Chierici, F., Sartori, R. and Torelli, L. 1999. The tectonic source of the 1755 Lisbon earthquake and tsunami. *Annali di Geofisica* 42(1).

Zitellini, N., Mendes, L.A., Córdoba, D., Dañobeitia, J.J., Nicolich, R., Pellis, G., Ribeiro, G., Sartori, R., Torelli, L., et al., 2001. Source of 1755 Lisbon earthquake and tsunami investigated. *EOS, Trans. Am. Geophys*. Union 82, 285–291.

Zitellini, N., Rovere, M., Terrinha, P., Chierici, F., Matias, L., Team, B., 2004. Neogene through Quaternary tectonic reactivation of SW Iberian passive margin. *Pure Appl. Geophys*. 161, 565–587. doi:10.1007/s00024-003-2463-4.

Zitellini, N., E. Gràcia, M.A. Gutscher, L. Matias, D. Masson, T. Mulder, P. Terrinha, L. Somoza, G. DeAlteriis, J.P. Henriet, J.J. Dañobeitia, R. Ramella, M.A. Abreu and S. Diez. (in prep.). The quest for the Iberia-Africa Plate boundary west of Gibraltar, *Science*, in prep., 2008.